NATIONAL ADVISORY COMMITTEE FOR AERONAUTICS

REPORT No. 585

SPAN LOAD DISTRIBUTION FOR TAPERED WINGS WITH PARTIAL-SPAN FLAPS

By H. A. PEARSON

1937

For sale by the Superintendent of Documents, Washington, D. C. - - - - - - - - - - - - - Price 10 cents

AERONAUTIC SYMBOLS

1. FUNDAMENTAL AND DERIVED UNITS

	Symbol	Metric		English	
		Unit	Abbreviation	Unit	Abbreviation
Length	l	meter	m	foot (or mile)	ft. (or mi.)
Time	t	second	s	second (or hour)	sec. (or hr.)
Force	F	weight of 1 kilogram	kg	weight of 1 pound	lb.
Power	P	horsepower (metric)		horsepower	hp.
Speed	V	{kilometers per hour {meters per second	k.p.h. m.p.s.	miles per hour feet per second	m.p.h. f.p.s.

2. GENERAL SYMBOLS

W, Weight $=mg$

g, Standard acceleration of gravity $=9.80665$ m/s^2 or 32.1740 ft./sec.^{2}

m, Mass $=\frac{W}{g}$

I, Moment of inertia $=mk^2$. (Indicate axis of radius of gyration k by proper subscript.)

μ, Coefficient of viscosity

ν, Kinematic viscosity

ρ, Density (mass per unit volume)

Standard density of dry air, 0.12497 kg-m^{-4}-s^2 at 15° C. and 760 mm; or 0.002378 lb.-ft.$^{-4}$ sec.^{2}

Specific weight of "standard" air, 1.2255 kg/m^3 or 0.07651 lb./cu.ft.

3. AERODYNAMIC SYMBOLS

S, Area

S_w, Area of wing

G, Gap

b, Span

c, Chord

$\frac{b^2}{S}$ Aspect ratio

V, True air speed

q, Dynamic pressure $=\frac{1}{2}\rho V^2$

L, Lift, absolute coefficient $C_L=\frac{L}{qS}$

D, Drag, absolute coefficient $C_D=\frac{D}{qS}$

D_o, Profile drag, absolute coefficient $C_{D_o}=\frac{D_o}{qS}$

D_i, Induced drag, absolute coefficient $C_{D_i}=\frac{D_i}{qS}$

D_p, Parasite drag, absolute coefficient $C_{D_p}=\frac{D_p}{qS}$

C, Cross-wind force, absolute coefficient $C_C=\frac{C}{qS}$

R, Resultant force

i_w, Angle of setting of wings (relative to thrust line)

i_t, Angle of stabilizer setting (relative to thrust line)

Q, Resultant moment

Ω, Resultant angular velocity

$\rho\frac{Vl}{\mu}$, Reynolds Number, where l is a linear dimension (e.g., for a model airfoil 3 in. chord, 100 m.p.h. normal pressure at 15° C., the corresponding number is 234,000; or for a model of 10 cm chord, 40 m.p.s. the corresponding number is 274,000)

C_p, Center-of-pressure coefficient (ratio of distance of *c.p.* from leading edge to chord length)

α, Angle of attack

ϵ, Angle of downwash

α_o, Angle of attack, infinite aspect ratio

α_i, Angle of attack, induced

α_a, Angle of attack, absolute (measured from zero-lift position)

γ, Flight-path angle

REPORT No. 585

SPAN LOAD DISTRIBUTION FOR TAPERED WINGS WITH PARTIAL-SPAN FLAPS

By H. A. PEARSON

Langley Memorial Aeronautical Laboratory

129029—37——1

NATIONAL ADVISORY COMMITTEE FOR AERONAUTICS

HEADQUARTERS, NAVY BUILDING, WASHINGTON, D. C.

LABORATORIES, LANGLEY FIELD, VA.

Created by act of Congress approved March 3, 1915, for the supervision and direction of the scientific study of the problems of flight. Its membership was increased to 15 by act approved March 2, 1929. The members are appointed by the President, and serve as such without compensation.

TECHNICAL COMMITTEES

AERODYNAMICS
POWER PLANTS FOR AIRCRAFT
AIRCRAFT STRUCTURES AND MATERIALS
AIRCRAFT ACCIDENTS
INVENTIONS AND DESIGNS

Coordination of Research Needs of Military and Civil Aviation

Preparation of Research Programs

Allocation of Problems

Prevention of Duplication

Consideration of Inventions

LANGLEY MEMORIAL AERONAUTICAL LABORATORY

LANGLEY FIELD, VA.

Unified conduct, for all agencies, of scientific research on the fundamental problems of flight.

OFFICE OF AERONAUTICAL INTELLIGENCE

WASHINGTON, D. C.

Collection, classification, compilation, and dissemination of scientific and technical information on aeronautics.

REPORT No. 585

SPAN LOAD DISTRIBUTION FOR TAPERED WINGS WITH PARTIAL-SPAN FLAPS

By H. A. Pearson

SUMMARY

Tables are given for determining the load distribution of tapered wings with partial-span flaps placed either at the center or at the wing tips. Seventy-two wing-flap combinations, including two aspect ratios, four taper ratios, and nine flap lengths, are included. The distributions for the flapped wing are divided into two parts, one a zero lift distribution due primarily to the flaps and the other an additional lift distribution due to an angle of attack of the wing as a whole.

Comparisons between theoretical and experimental results for wings indicate that the theory may be used to predict the load distribution with sufficient accuracy for structural purposes.

Simple computing forms are included for determining, by the Lotz method, the theoretical loadings for a combination of any wing with any flap. A discussion of the method is given showing: (1) the effect on the load distribution of increasing the number of harmonics for a wing with partial-span flaps; and (2) the effect of increasing the number of points used across the semispan for a wing of unfair plan form.

INTRODUCTION

A knowledge of the span load distribution over a wing is important not only from structural considerations but also because certain conclusions regarding the behavior of the wing near the stall may be drawn from it. Indirectly, the span load distribution also influences such items relating to performance as the magnitude of the induced drag, the pitching moment of the entire wing about an aerodynamic center, and the angle of zero lift. Because of the importance of span load distribution, numerous methods for computing it have been proposed but, since they are generally lengthy and complicated, they have been little used in practice.

In reference 1 the span loading was given for linearly tapered wings with rounded tips. The results given therein cover a large range of aspect ratios and taper ratios, but they are for the case of a wing in which there is either no twist or only linear twist. Since most airplanes include some sort of high-lift or drag-increasing device covering only part of the span, the wing with an abrupt twist is of particular interest. These high-lift devices, when deflected, may be considered as introducing an effective twist that alters the load distribution along the span. As the actual effective twist depends upon possible combinations of wing angle of attack, flap type, flap deflection, flap span, wing plan form, and the variation of the flap-chord ratio along the span, it is apparent that the resulting load distribution depends upon many variables.

The presence of so many variables precludes the possibility of making either sufficiently extensive theoretical or experimental investigations to provide design charts for the general case. The present report therefore covers only the most commonly used series of wings; i. e., linearly tapered wings with rounded tips having chord distributions like those of reference 1 and equipped with partial-span flaps of constant flap-chord ratio. Comparisons are made of the experimental loadings, taken from reference 2, and the theoretical loadings to give an indication of the differences to be expected when the theory is used. Finally, a method for computing the span loading is included so that those interested will be in a position either to estimate from the results given herein the probable loading for similar cases or, if necessary, actually to make the computations.

Although the present report presents only the span loadings, later reports will deal with the effect of the load distribution on performance and on the behavior of the wing near the stall.

SYMBOLS

b_f, flap span.
b_w, wing span.
S, wing area.
A, aspect ratio, b_w^2/S.
δ_f, flap deflection, positive downward.
V, wind velocity.
ρ, mass density of air.
q, dynamic pressure, $\frac{1}{2}\rho V^2$.
w, induced downflow at a section.
L, lift on wing.
C_L, wing lift coefficient, L/qS.
c_s, chord at plane of symmetry.
c, chord at any section.

α_0, effective angle of attack of any section.
α_a, angle of attack of any section referred to its zero-lift direction.
α_s, angle of attack of section at plane of symmetry referred to its zero-lift direction.
λ, ratio of fictitious tip chord, obtained by extending leading and trailing edges of wing to extreme tip, to the chord at the plane of symmetry.
E, ratio of flap chord to wing chord at any section.
Γ, circulation at a section.
l, section lift (per unit length along span).
c_l, section lift coefficient, l/qc, perpendicular to wind at infinity.
Subscripts:
- 0, refers to section lift coefficient perpendicular to local relative wind.
- b, refers to basic lift ($C_L=0$).
- a, refers to additional lift for any C_L.
- $a1$, refers to additional lift for $C_L=1.0$.

$c_{l_{max}}$, maximum lift coefficient for any section.
Δc_l, increment in section lift coefficient caused by a flap deflection, δ_f.
c_{d_i}, section induced-drag coefficient.
c_{d_0}, section profile-drag coefficient.
L_a, additional-load parameter, $c_{l_{a1}}\frac{cb}{S}$.
L_b, basic-load parameter, $c_{l_b}\frac{cb}{S\Delta c_l}$.
m, $\frac{dC_L}{d\alpha}$ of entire wing, per radian.
m_0, $\frac{dc_l}{d\alpha_0}$ of any section, per radian.
m_s, $\frac{dc_l}{d\alpha_0}$ of section at plane of symmetry, per radian.
ΔC_L, the part of C_L at a given wing attitude due to any flap deflection.
ΔC_{L_1}, the increment caused by a flap deflection corresponding to a Δc_l of 1.0.
y, variable point along span.
y', fixed point along span.
$\cos\theta$, $\frac{y}{b_w/2}$ (when $y=-b_w/2$, $\theta=0$; when $y=b_w/2$, $\theta=\pi$).
A_n, B_n, C_{2n}, coefficients in Fourier series.

THEORETICAL RESULTS FOR WINGS WITH FLAPS

According to the assumptions upon which wing theory is based, the distribution of lift over the span is a linear function of the angle of attack at each point of the span. Thus it is permissible to compute separately either a zero lift distribution or a distribution due only to the flaps and later to superpose them on appropriate distributions due to an angle of attack of the wing with flaps neutral.

Deflecting flaps on an untwisted wing that previously was at zero lift produces the angle of attack and load distributions shown by the solid lines in figure 1. If the angle of attack of the wing without flaps is reduced so that the area under the dashed load curve is equal to that under the solid curve, their addition will result in a zero-lift curve. It can be seen that the load distribution due to the flap alone (solid curve) does not follow

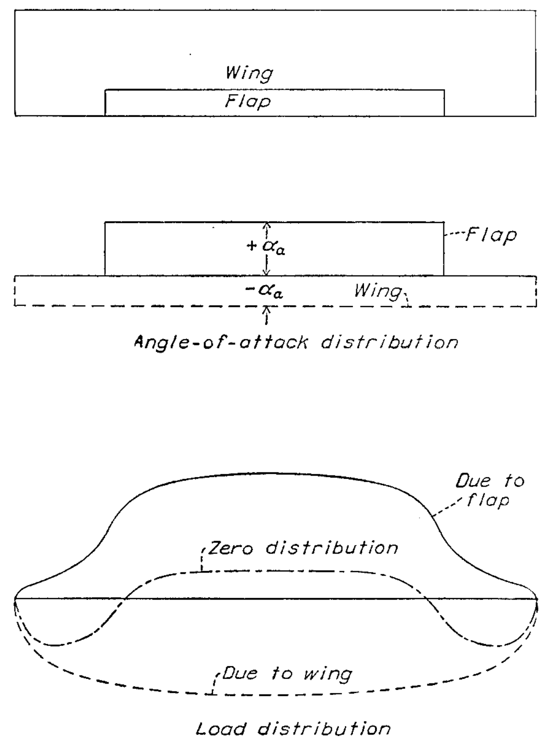

FIGURE 1.—Angle of attack and load distribution for a wing with flaps.

the abrupt angle-of-attack change but, owing to induction, is distributed along the remainder of the span where there is no apparent angle of attack. At these stations there is, however, an effective angle of attack due to the upwash produced by the portion with flaps. Numerically the effective angle of attack at any section is equal to the section c_l divided by the slope of the section lift curve, or it can be given by

$$\alpha_0=\alpha_a-\frac{w}{V} \quad (1)$$

In order to determine the theoretical distribution of the forces and angles for a particular case, it is necessary to obtain a solution of the fundamental formula for induced downflow

$$w=\frac{1}{4}\pi\int_{-\frac{b}{2}}^{\frac{b}{2}}\frac{\frac{d\Gamma}{dy}dy}{y'-y} \quad (2)$$

The graphical and analytical methods for solving this complicated integral tend to be lengthy and none is exact. In the general case where the wing plan form or angle-of-attack distribution cannot be expressed as simple analytical functions, either the Lotz or Lippisch methods (references 3 and 4) are particularly applicable, although other methods may be used. An adaptation of the Lotz method, which has been used to compute the theoretical load distributions given herein, is given in a later section of this report in a form suitable for routine computation. These load distributions are listed in tables I and II for 72 wing-flap combinations that include two aspect ratios (6 and 10), four taper ratios (1.0, 0.75, 0.50, and 0.25), and nine flap lengths. The flap lengths, expressed as a fraction of the semispan, are:

Flaps at center	Flaps at tip
0.233	0.240
.383	.351
.649	.617
.760	.767
1.000	-----

Table I gives the ordinates of the curves of the additional load distribution at 10 selected spanwise stations in terms of the parameter

$$L_a = c_{l_{a1}} \frac{cb}{S} \tag{3}$$

and table II gives the ordinates for the basic-load distribution in terms of the parameter

$$L_b = c_{l_b} \frac{cb}{S\Delta c_l} \tag{4}$$

The additional-load distribution, given for a wing C_L of 1.0, is independent of wing twist (flap displacement) and maintains the same form throughout the useful range of the lift curve. The basic distributions are zero lift distributions that depend principally on the wing twist.

The values of L_a and L_b were computed by the Lotz method; 10 points across the semispan were used and 10 harmonics of the series were retained. In these computations the slope of the section lift curve was assumed to be equal to 5.67. The odd flap lengths given result from the use of a Fourier series in the solution for the load curves; in the case of a wing with an abrupt twist the discontinuity occurs, mathematically, in the interval including the end of the flap.

Since the parameter L_a has been given for the convenient wing C_L of 1.0, the relation between the additional section lift coefficients c_{l_a} and $c_{l_{a1}}$ becomes

$$c_{l_a} = C_L c_{l_{a1}} \tag{5}$$

The total lift coefficient at each section is

$$c_l = c_{l_b} + C_L c_{l_{a1}} \tag{6}$$

and the lift at a section is

$$l = c_l q c \tag{7}$$

In the application of the results given in tables I and II, interpolation will generally be necessary. For structural purposes a linear interpolation between the different variables is probably justified. The results may also be extrapolated with reasonable accuracy to aspect ratios 4 and 12, although values of L_a may be obtained from reference 1 for aspect ratios from 3 to 20 without the necessity of any extrapolation.

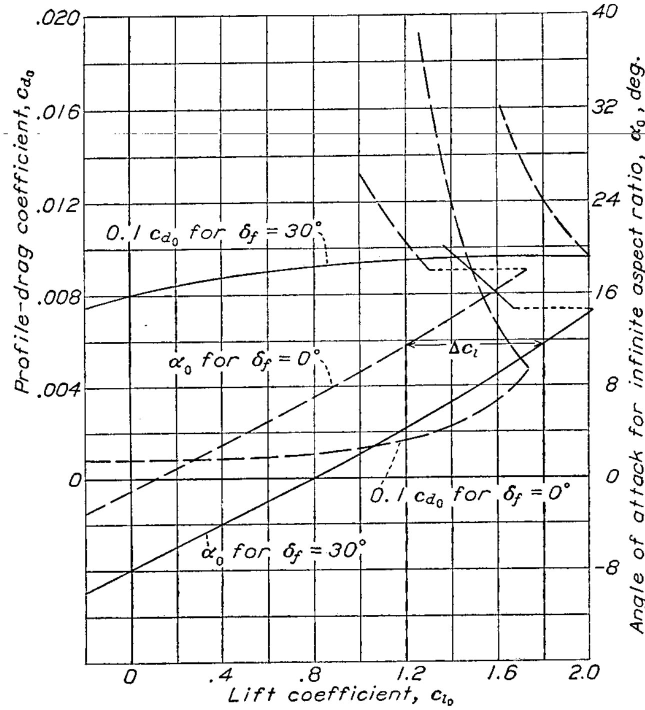

FIGURE 2.—Typical characteristics of a section equipped with a flap.

In order to illustrate the procedure to be followed in the use of the tables, the span loading of a wing with the following characteristics will be found:

$C_L = 1.72$
$\lambda = 0.625$
$A = 6$
$\frac{b_f}{b_w} = 0.383.$
$q = 57.5$ pounds per square foot
$E = 0.20$
$\delta_f = 30°$

A table, such as table III, is prepared in which the values of the chord at the various stations are first entered, interpolations are made for taper, etc., and the values of L_a and L_b from tables I and II are entered in columns 3 and 4, respectively. From L_a, the values of $c_{l_{a1}}$ and c_{l_a} are found by the use of equations (3) and (5) and entered in columns 5 and 6.

Before c_{l_b} can be found, however, it is necessary to determine from experimental data the value of Δc_l corresponding to the flap-displacement angle of 30°. This increment is generally found by correcting the results of tests made of a finite wing with full-span flaps of proper type and proper flap-chord ratio to obtain section characteristics. It is assumed that such section characteristics are available (fig. 2); the value of Δc_l to be used may then readily be found. Theoretically,

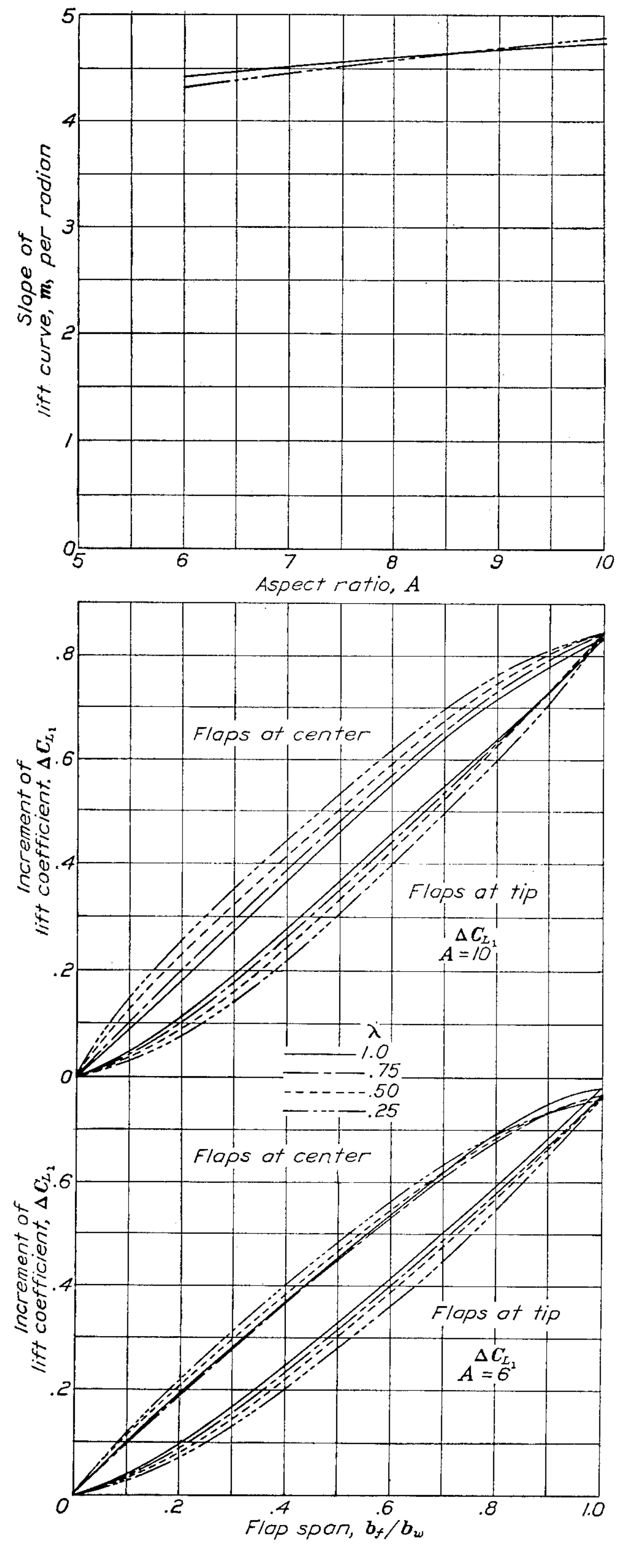

FIGURE 3.—Values of lift increments and lift-curve slopes for wings with partial-span flaps.

the effect of displacing a flap would be to displace the lift curves parallel to each other so that Δc_l would be independent of the effective angle of attack. Experimental results, however, indicate that Δc_l depends on the effective angle of attack and some averaging is thus necessary to determine its value. Since the example is for a high-angle-of-attack condition, the value of Δc_l is arbitrarily taken in this range at an angle corresponding to a c_l of 1.2 for the plain section. By the use of equation (4) together with a value of Δc_l equal to 0.6, from figure 2, the values of c_{l_b} are computed and entered in column 7 of table III. The total section c_l (column 8), from which the load distribution (column 9) is determined, is the sum of columns 6 and 7.

Standard section characteristics for the plain section and the section with a flap are sometimes tabulated instead of being plotted as in figure 2. In such a case the value of Δc_l may be found from the formula

$$\Delta c_l = c_{l_f}\left(1-\frac{a_0}{a_{0_f}}\right) + a_0\left(\alpha_{l_0} - \alpha_{l_{0_f}}\right)$$

where α_0 is the slope of the section lift curve per degree and α_{l_0} the angle of zero lift measured from the chord line in degrees. The subscript f refers to the characteristics with the flap deflected. If desired, the slopes and angles could also be given in radians.

If the induced-drag distribution corresponding to a given load distribution is specifically required, it may be found by the use of the equation

$$c_{d_i} = c_l\left[\left(\frac{C_L - \Delta C_{L_1}\Delta c_l}{m}\right) - \frac{c_l}{m_0}\right] \qquad (8)$$

which gives the variation of the section induced-drag coefficient over the portion of the span without flaps, and the equation

$$c_{d_i} = c_l\left[\left(\frac{C_L - \Delta C_{L_1}\Delta c_l}{m}\right) + \left(\frac{\Delta c_l - c_l}{m_0}\right)\right] \qquad (9)$$

which holds over the portion of the span with flaps. The increment of wing lift coefficient ΔC_{L_1} and the slope of the lift curve of the finite wing m to be used in these equations are given in figure 3 for the series of wings considered in this report. The value of ΔC_{L_1} (fig. 3) represents the increase in lift coefficient based on the entire wing area due to a flap deflection corresponding to a Δc_l of 1.0. Figure 4 gives typical distributions of $c_l\frac{cb}{S}$ and c_l for various wing-flap combinations corresponding to a Δc_l of 1.0. These distributions are thus directly related to the results given in figure 3.

COMPARISONS OF EXPERIMENTAL AND THEORETICAL RESULTS

Previous comparisons (reference 5) of experimental and theoretical span loadings for a 2:1 tapered U. S. A. airfoil equipped with partial-span flaps of three different lengths indicated a satisfactory agreement. The first conclusion given in reference 5 is: "A satisfactory determination, for all conditions of test, of the span load distribution for an airfoil equipped with a partial-span split flap may be made by applying the Lotz method of calculating the aerodynamic characteristics of wings. The increments of load due to the deflection of the flap are computed by the Lotz method and added to the span load distribution for the plain airfoil."

Since the publication of reference 5 additional pressure-distribution tests (reference 2) have been made over a rectangular wing having a 0.6-span constant-chord split flap. The wing used was of Clark Y section with a 20-inch chord and a total span of 120 inches. Some of the span-loading curves taken from reference 2 are compared, in figure 5, with corresponding theoretical curves for a wing with square tips.

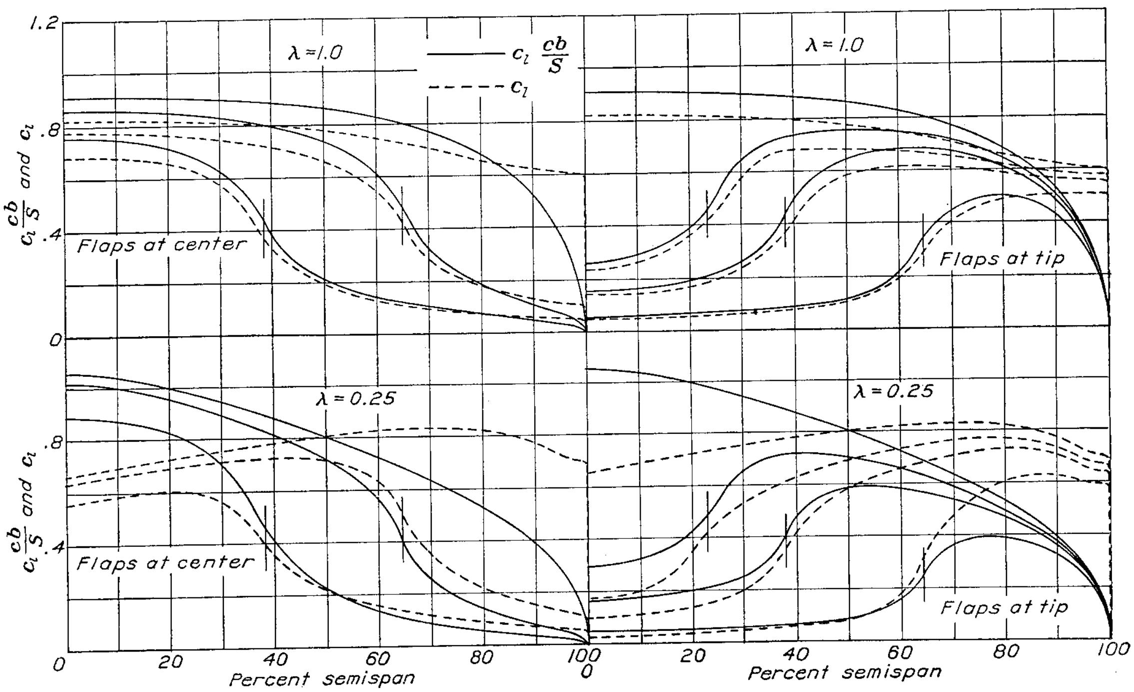

FIGURE 4.—Typical distributions of $c_l \frac{cb}{S}$ and c_l due to a flap deflection. ($A=6$; $\Delta c_l=1.0$.)

Figure 6 shows comparisons of computed and experimental values of ΔC_L for various flap locations. The experimental values of ΔC_L are those given in references 6 and 7 at 8° angle of attack. Reference 6 gives the results of force tests of a rectangular Clark Y wing with partial-span flaps placed at the center and at the wing tips; reference 7 gives similar results for a 5:1 tapered wing. In the comparisons given in figure 6 the experimental results were obtained from tests of wings with straight tips; whereas the computed results are those for wings with rounded tips.

THE LOTZ METHOD FOR CALCULATING THE AERODYNAMIC CHARACTERISTICS OF WINGS

The following method was proposed in 1931 by Miss Lotz (reference 3), who gave the basic theory involved. Shenstone (reference 8) gave a brief discussion of the method and a simple procedure to be used in obtaining the various constants required in the solution. In this section the method will be discussed in more detail and a series of computing forms will be given which, it is believed, will make the computations simpler and more direct than if the method of reference 8 were followed.

Outline of theory.—As is customary in aerodynamic theory, the wing is replaced by a single line vortex whose strength at every section along the span is equal to the circulation Γ at that section. The lift per unit length of span is then

$$dL=\rho V\Gamma dy \tag{10}$$

and the problem is to find Γ for any point on a wing of any shape. The relations between Γ, c_l, and α_0 are given by the equations

$$\Gamma=\frac{c_l cV}{2}-\frac{\alpha_0 m_0 cV}{2} \tag{11}$$

where $\alpha_0=\alpha_a-w/V$. Since the induced angle at a particular station y' is

$$\frac{w}{V}=\frac{1}{4\pi V}\int_{-\frac{b}{2}}^{\frac{b}{2}}\frac{\frac{d\Gamma}{dy}}{y'-y}dy \tag{12}$$

the circulation Γ may be expressed by the integral equation

$$\frac{2\Gamma}{m_0 cV}=\alpha_a-\frac{1}{4\pi V}\int_{-\frac{b}{2}}^{\frac{b}{2}}\frac{\frac{d\Gamma}{dy}}{y'-y}dy \tag{13}$$

This equation is to be solved for Γ, and the method used is to replace the circulation by a Fourier series where

$$\Gamma=\frac{c_s m_s V}{2}\Sigma A_n \sin n\theta \tag{14}$$

and hence

$$\frac{2\Gamma}{m_0 c V}=\frac{m_s}{m_0}\frac{c_s}{c}\Sigma A_n \sin n\theta \tag{15}$$

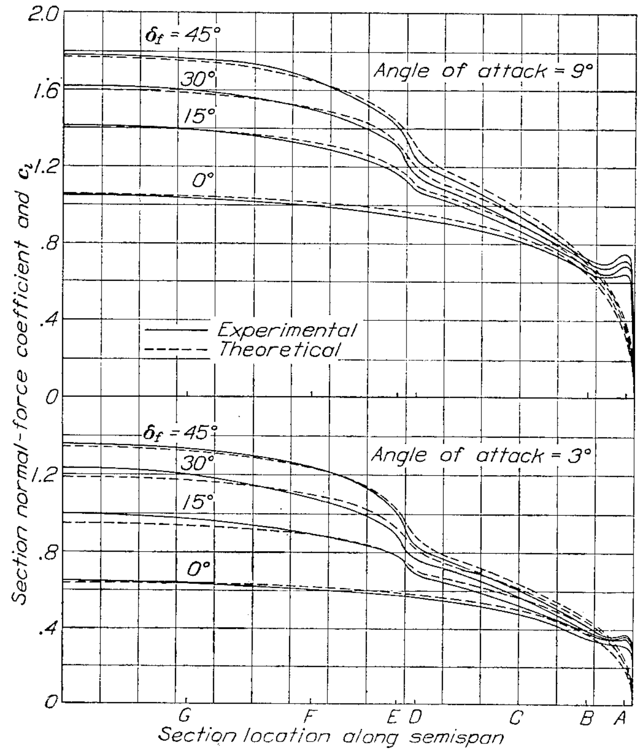

FIGURE 5.—Comparison between experimental and theoretical load distribution for a wing with partial-span flaps. (Data from reference 2; λ=1.0; A=6; square tips.)

As a result of expressing the circulation by the foregoing series, the induced angle becomes

$$\frac{w}{V}=\frac{c_s\, m_s}{4b}\Sigma nA_n\left(\frac{\sin n\theta}{\sin\ \theta}\right) \tag{16}$$

By substitution, equation (13) is transformed into

$$\frac{m_s}{m_0}\frac{c_s}{c}\sin\theta\ \Sigma A_n \sin n\theta=\alpha_a \sin\theta-\frac{c_s m_s}{4b}\Sigma nA_n \sin n\theta \tag{17}$$

The new feature introduced by Miss Lotz is to replace $\frac{m_s}{m_0}\frac{c_s}{c}\sin\theta$ and $\alpha_a \sin\theta$ by the two series $\Sigma C_{2n}\cos 2n\theta$ and $\Sigma B_n \sin n\theta$, respectively. As the coefficients in these series are independent of the load distribution, they may be separately computed, and it is possible to increase the accuracy by taking more terms without changing the values of the coefficients already computed. When the wing plan form is symmetrical about the center line, the cosine series contains only even values; whereas, if the angle-of-attack distribution is symmetrical, as it is with flaps, only odd values of n are retained. Equation (17), after the foregoing series have been substituted, becomes

$$\Sigma C_{2n}\cos 2n\theta\ \Sigma A_n \sin n\theta+\frac{c_s m_s}{4b}\Sigma nA_n \sin n\theta= \Sigma B_n \sin n\theta \tag{18}$$

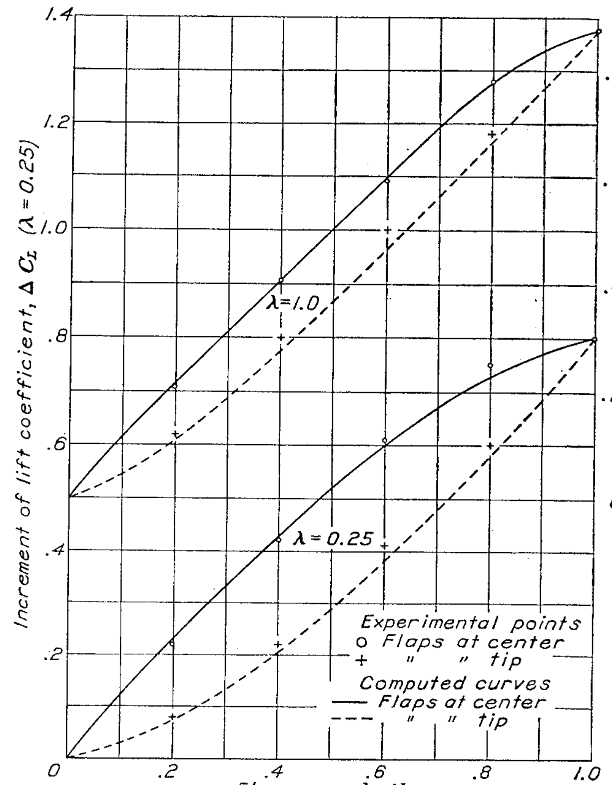

FIGURE 6.—Comparison of experimental and computed values of ΔC_L.

When n is temporarily replaced by the indices k and l, the double series on the left of equation (18) is transformed into

$$\tfrac{1}{2}\sum_k\sum_l A_k\, C_l[\sin\ (k+l)\theta+\sin\ (k-l)\theta]$$

By the substitution of the foregoing series and considerable rearrangement, equation (18) may be expanded into the following form. In its exact form there are an infinite number of equations and terms. For the purpose of calculation, however, the circulation may be computed at a finite number of points with a finite number of equations.

A B C

$$
\left.
\begin{aligned}
&2P_1A_1+(C_2-C_4)A_3+(C_4-C_6)A_5+(C_6-C_8)A_7+(C_8-C_{10})A_9+(C_{10}-C_{12})A_{11}+(C_{12}-C_{14})A_{13}+(C_{14}-C_{16})A_{15}+(C_{16}-C_{18})A_{17}+(C_{18}-C_{20})A_{19}=2B_1\\
&(C_2-C_4)A_1+2P_3A_3+(C_2-C_8)A_5+(C_4-C_{10})A_7+(C_6-C_{12})A_9+(C_8-C_{14})A_{11}+(C_{10}-C_{16})A_{13}+(C_{12}-C_{18})A_{15}+(C_{14}-C_{20})A_{17}+(C_{16}-C_{22})A_{19}=2B_3\\
&(C_4-C_6)A_1+(C_2-C_8)A_3+2P_5A_5+(C_2-C_{12})A_7+(C_4-C_{14})A_9+(C_6-C_{16})A_{11}+(C_8-C_{18})A_{13}+(C_{10}-C_{20})A_{15}+(C_{12}-C_{22})A_{17}+(C_{14}-C_{24})A_{19}=2B_5\\
&(C_6-C_8)A_1+(C_4-C_{10})A_3+(C_2-C_{12})A_5+2P_7A_7+(C_2-C_{16})A_9+(C_4-C_{18})A_{11}+(C_6-C_{20})A_{13}+(C_8-C_{22})A_{15}+(C_{10}-C_{24})A_{17}+(C_{12}-C_{26})A_{19}=2B_7\\
&(C_8-C_{10})A_1+(C_6-C_{12})A_3+(C_4-C_{14})A_5+(C_2-C_{16})A_7+2P_9A_9+(C_2-C_{20})A_{11}+(C_4-C_{22})A_{13}+(C_6-C_{24})A_{15}+(C_8-C_{26})A_{17}+(C_{10}-C_{28})A_{19}=2B_9\\
&(C_{10}-C_{12})A_1+(C_8-C_{14})A_3+(C_6-C_{16})A_5+(C_4-C_{18})A_7+(C_2-C_{20})A_9+2P_{11}A_{11}+(C_2-C_{24})A_{13}+(C_4-C_{26})A_{15}+(C_6-C_{28})A_{17}+(C_8-C_{30})A_{19}=2B_{11}\\
&(C_{12}-C_{14})A_1+(C_{10}-C_{16})A_3+(C_8-C_{18})A_5+(C_6-C_{20})A_7+(C_4-C_{22})A_9+(C_2-C_{24})A_{11}+2P_{13}A_{13}+(C_2-C_{28})A_{15}+(C_4-C_{30})A_{17}+(C_6-C_{32})A_{19}=2B_{13}\\
&(C_{14}-C_{16})A_1+(C_{12}-C_{18})A_3+(C_{10}-C_{20})A_5+(C_8-C_{22})A_7+(C_6-C_{24})A_9+(C_4-C_{26})A_{11}+(C_2-C_{28})A_{13}+2P_{15}A_{15}+(C_2-C_{32})A_{17}+(C_4-C_{34})A_{19}=2B_{15}\\
&(C_{16}-C_{18})A_1+(C_{14}-C_{20})A_3+(C_{12}-C_{22})A_5+(C_{10}-C_{24})A_7+(C_8-C_{26})A_9+(C_6-C_{28})A_{11}+(C_4-C_{30})A_{13}+(C_2-C_{32})A_{15}+2P_{17}A_{17}+(C_2-C_{36})A_{19}=2B_{17}\\
&(C_{18}-C_{20})A_1+(C_{16}-C_{22})A_3+(C_{14}-C_{24})A_5+(C_{12}-C_{26})A_7+(C_{10}-C_{28})A_9+(C_8-C_{30})A_{11}+(C_6-C_{32})A_{13}+(C_4-C_{34})A_{15}+(C_2-C_{36})A_{17}+2P_{19}A_{19}=2B_{19}
\end{aligned}
\right\}
\tag{19}
$$

$$P_n=C_0-\frac{1}{2}C_{2n}+n\frac{c_sm_s}{4b}$$

These equations form a system of normal simultaneous equations, and it will be seen later that in the nth equation the unknown A_n has the greatest coefficient, the others decreasing rather rapidly. Because of this circumstance, the system is most easily solved by a method of successive approximations.

In the first equation, since the value of all the terms is small compared with $P_1\,A_1$, an approximation to A_1 is obtained by assuming all terms except A_1 equal to zero. Then in the next equation, since $P_3\,A_3$ is large with respect to all terms except $(C_2-C_4)\,A_1$, which is known, an approximation to A_3 is obtained by assuming the remaining terms equal to zero. Thus by the substitution of the approximated values in the other equations, approximate values of the remaining coefficients are obtained which, when substituted back in the first equation, result in a closer approximation for A_1. A repetition results in closer approximations for all the coefficients. In this way the process can be carried on until the approximations of the coefficients cease to differ. Usually the second approximation is fairly close, and the third may be considered as exact. (See illustrative example.)

Forms for computing B_n and C_{2n} coefficients.—Before the system of simultaneous equations (19) can be solved, the B_n and C_{2n} coefficients must be found. Forms for determining these coefficients are given by plates I to IV, inclusive. Plates I and II are for the case when the circulation is to be determined at 10 points across the semispan and plates III and IV are for 20 points.

It is only necessary to tabulate on each of the forms the values of y_n and y_n' and to follow the steps indicated. The values of y_n are the ordinates for the $\alpha\sin\theta$ curves taken either every 9° or 4½° (starting with the tip as zero), depending upon whether 10 or 20 points are used. The values of y_n' are the ordinates of the $\frac{m_s}{m_0}\frac{c_s}{c}\sin\theta$ curves taken at the same intervals as before. The checks indicated at the bottoms of these forms merely serve as checks of the numerical work performed on that sheet and, if only a few harmonics are to be retained, the arithmetic may be decreased by computing only the coefficients necessary and omitting the checks.

Number of harmonics or points to be retained.—In the series of simultaneous equations given by equation (19) the question naturally arises as to how many equations should be used and how many points across the semispan are required. The system shown is for 10 points, but it may easily be extended to more than 10 points by following the indicated trend. In the case given (equation (19)), the conditions are satisfied at only 10 points when the whole system of equations is solved simultaneously; if the system is cut off, as at A, B, or C, where 4, 5, and 8 harmonics are retained, the circulation may still be found at 10 points but with a greater degree of approximation.

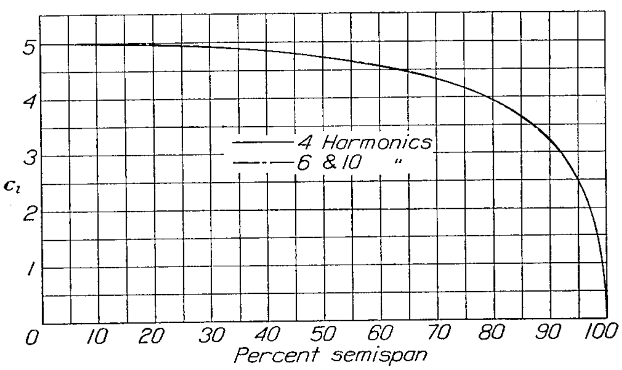

FIGURE 7.—Effect of the number of harmonics on the span of c_l distribution of a wing without flaps. (Angle of attack, α, 1 radian.)

As a criterion for gaging the number of harmonics to be retained, the span c_l distribution has been computed (fig. 7) for an untwisted rectangular wing (straight tips) of aspect ratio 6 at 1 radian angle of attack, using 4, 6, and 10 harmonics. The calculations were repeated (fig. 8) for the same wing with a $\frac{b_f}{b_w}=0.649$ flap extending out from the center. The angle of attack for the portion with flap is 1 radian and that of the remainder of the wing is zero. In both cases 10 points have been used across the semispan. The A_n, or circulation, coefficients from which the distributions of figures 7 and 8 were computed are given in table IV. In figure 9 the distribution has been computed for a wing with double taper. Distributions are given for the case using 10 points and retaining 4 and 10 harmonics of the series and also for the case with 20 points and 4 harmonics. For convenience the distributions have been computed for an untwisted wing at an angle of attack of 1 radian.

Example.—In order to illustrate the method of calculating the wing characteristics, an example for a wing with partial-span flaps is worked through the forms to determine the B_n and C_{2n} coefficients. The calculations are made for one of the wing shapes given in this report ($\lambda=0.50$, $A=10$, $b_f/b_{cr}=0.489$) at an angle of attack of 1 radian from 0 to 0.489 and 0 from 0.489 to 1.0. The additional types of forms and tables necessary to compute the load distribution for a given case are also included.

Table V is a tabulation of the known geometric quantities of the wing for which the load distribution is desired. Column 1 of this table merely designates the points along the span, the numbers increasing

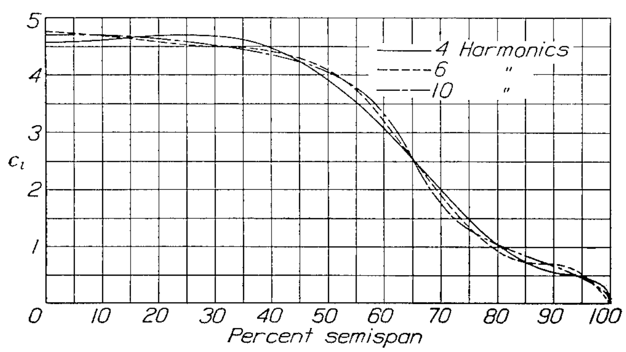

FIGURE 8.—Effect of the number of harmonics on the span c_l distribution of a wing with flaps. (Angle of attack, 1 radian from 0 to 0.649 and 0 from 0.649 to 1.000.)

numerically from the wing tip; column 5 represents the angle of attack measured from zero lift at the points along the span given in column 2. Where an abrupt twist exists, the discontinuity will fall within the portions of the span given in column 2. The final computations, however, will be for the case of a flap whose end lies halfway between these points. Because of this fact a slight discrepancy in length may occur, which can be reduced by increasing the number of points. In the present case only the distribution due to the flaps is found. In order to obtain a complete determination of the distribution at other flap angles and wing angles, it would also be necessary to find the distribution corresponding to the plain wing. For this case the C_{2n} coefficients remain unchanged and $B_1=\alpha_s$, all other B_n values being zero. Column 7 is the slope of the section lift curves along the span which, in this case, is assumed as 5.67. Column 8 is the ratio of the slope of the section at the plane of symmetry to the slopes of the sections at each station. Column 9 is the ratio of the chord at the plane of symmetry to the chord at each section.

The values of columns 6 and 10 (y_n and y_n') are then tabulated as shown in table VI and the instructions of plates I and II, or of plates III and IV as in the present example, are followed until the B_n and C_{2n} coefficients are found. If this method were used and only four harmonics were to be retained, it would be only necessary to compute B_1 to B_7 and C_0 to C_{14} (see A, equation (19)); computing the remaining coefficients would be necessary only to obtain the check.

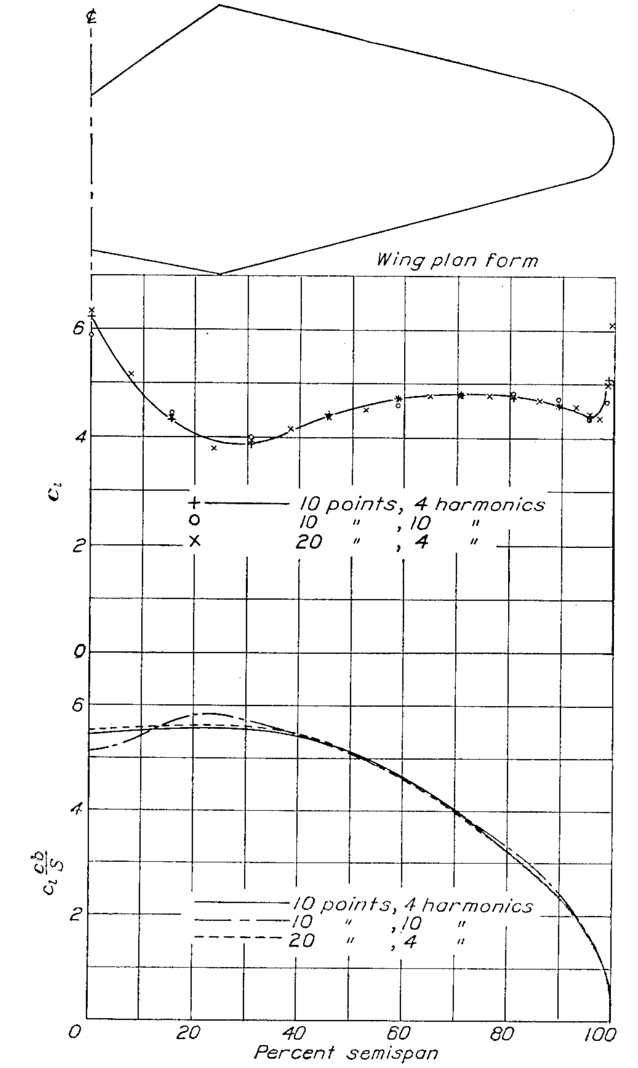

FIGURE 9.—Effect of the number of points and harmonics on the span c_l distribution for a wing with double taper.

A calculating form similar to table VII is then prepared. This form, as given, is complete for the case of 10 harmonics irrespective of the number of points. It will be noted that each major horizontal division represents one of the simultaneous equations occurring in equation (19). In column 1 of table VII are given the operations required to obtain the coefficients and in column 2 are tabulated the values of the coefficients, etc., just found. In column 3 (a) are listed the values of the A_n coefficients when they are known. Since none are known at the start, A_1 is determined as though the others were absent and listed in column 4 (a). The value of A_3 is next approximated in the same way, except that the value of A_1 just found is used as indicated. The same procedure is followed for A_5, A_7, etc., and these values are listed in column 4 (a). After all the A_n's have been approximated in this way, they are written in column 3 (b) and the whole process repeated, using the latest approximated value for each coefficient as it appears. It can be seen that the third approximation shows very little change from the second, indicating that a solution has been obtained. If it is desired to use fewer equations and harmonics, the corresponding computing form can be obtained from the present table VII simply by omitting all computations dealing with the higher harmonics. Thus if four harmonics were retained only portions of the form between the braces would be retained and the computations would proceed as before.

It will be noted, in the present example, that, although the B_n and C_{2n} coefficients were determined for 20 points, it is not necessary that c_l be computed for every point to obtain the final load curve. Even though the computations of the load distribution may be somewhat shortened in this manner, the value of c_l should not be computed at points other than those first selected.

An examination of equation (19) will indicate that, if n harmonics are retained, n values of B and $2n$ values of C are required. Hence, if it were decided to use 10 harmonics and compute the circulation at 10 points, the B_n and C_{2n} values can be determined for 20 points and the process shortened as indicated, or the B_n coefficients could be determined from plate I and the C_{2n} coefficients from plate IV.

After the A_n coefficients have been determined, the c_l values (in the present case $c_l = c_{l_a}$) are found from

$$c_l = \frac{m_s c_s}{c} \Sigma A_n \sin n\theta \tag{20}$$

These computations for c_l are given in table VIII for only 10 points. The wing C_L is found from

$$C_L = \pi A \frac{m_s c_s}{4b} A_1 \tag{21}$$

When this value is known, the distribution at any other C_L is obtained by direct proportion.

If desired, the induced-drag distribution may also be computed by using the A_n coefficients

$$c_{d_i} = c_l \frac{m_s c_s}{4b} \sum \frac{n A_n \sin n\theta}{\sin \theta} \tag{22}$$

as shown in table VIII; however, an easier method would be to compute it at each point from the equation

$$c_{d_i} = c_l \left(\alpha - \frac{c_l}{m_0} \right) \tag{23}$$

DISCUSSION

Although the computed span-loading curves show a qualitative agreement with the experimental wing curves (fig. 5), it is not so good as might be inferred from the results for the 2:1 tapered wing of reference 5. In the present comparison, however, the disagreement at the tip may be somewhat discounted since the square tip on a rectangular wing is known to give a high tip load. Comparisons of experimental and theoretical distributions for plain wings have indicated better agreement either as the tip was rounded or as the value of λ was decreased.

Rib-pressure curves taken from reference 2 (fig. 10) show a drop in positive pressure near the trailing edge for a section just beyond the end of the flap. This loss in lift may partly account for the fact that the experimental distributions give sharper breaks than the corresponding computed curves. An improvement in the

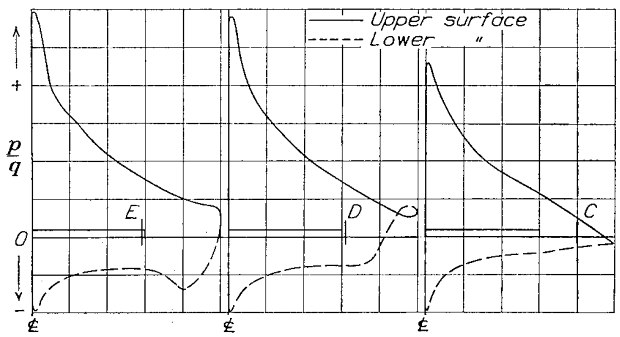

FIGURE 10.—Rib pressure distribution on a Clark Y wing with a partial-span split flap. (Reference 2; $\alpha=15°$; $\delta_f=45°$.)

agreement at the end of the flap may also be obtained by using more points and more harmonics in the series for deriving the theoretical distributions.

For the rest of the span the agreement between the computed and experimental curves would have been slightly improved if jet-boundary corrections had been applied to the data of reference 5. This correction, which varies along the wing span, would effect a better agreement in the present case.

The number of harmonics to be used in computing the span loading depends both on the wing plan form and on the type of wing twist. For wings with a continuous taper and twist, four harmonics may be sufficient (fig. 7); whereas, for wings with either a sharp double taper or a discontinuous twist, it may be necessary to increase the number of harmonics and points (figs. 8 and 9), depending, of course, upon the desired accuracy.

Although the data given herein are intended primarily for structural purposes, they may also be useful in relation to the stalling of tapered wings with flaps. When a partial-span flap is deflected, there is an increase in effective angle of attack and in the value of $c_{l_{max}}$ for the sections with the flap; whereas, for the sections beyond the flap, the effective angle of attack is theoretically increased without any increase in the value of $c_{l_{max}}$. Thus, according to lifting-line theory, the tip-stalling tendency of the tapered wing should be augmented by the use of flaps that extend out from the center, while the center-stalling tendency of the rectangular wing should be increased by flaps at the tips.

Experimental results from reference 2 (fig. 11), however, indicate that the pitching-moment coefficient (or effective camber) of sections considerably beyond the flap are actually increased by a flap deflection. This increase may prevent these outboard sections from stalling as early as would be indicated by the use of lifting-line theory. Furthermore, since theory neglects any transverse flow, any stalling characteristics based upon it may be at best only qualitatively correct. This statement is particularly true of a wing with a partial-span flap, where a relatively large transverse flow exists owing to the abrupt change in lift distribution produced by the flap. Lachmann's tests (reference 9), in which the action of wool tufts was observed, seem to indicate that the transverse flow delays the stall of sections immediately adjacent to the flap, thus causing the initial stalling point to move outward away from the flap end.

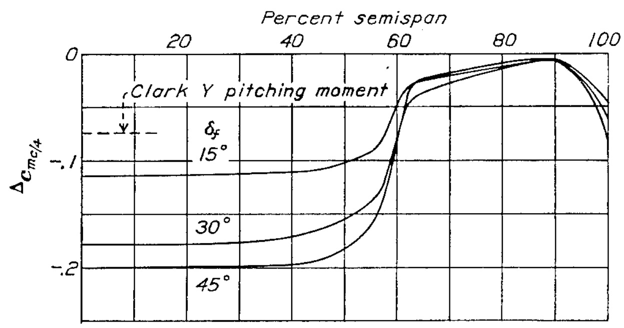

FIGURE 11.—Increment of pitching moment caused by deflecting a 0.6-span split flap on a rectangular Clark Y wing (reference 2).

In regard to the application of the calculations to structural design, fore-and-aft forces as well as vertical forces must be taken into account. An examination of equation (8) indicates that when $\Delta C_{L_1} \Delta c_l$ is equal to C_L (case given by solid lines in fig. 1) the portion of the wing without flaps has its lift vector displaced forward owing to the upflow produced by the flapped part. This forward component may be large enough to cancel the profile drag. Thus, for a wing with flaps at the center, the drag force is concentrated over the flap portion, and there may be an antidrag force over the outer portion of the wing. Hence, in design these conditions should be taken into account in some rational manner.

For structural purposes the c_l values obtained by use of tables I and II, or by computations, may be considered equal to c_{l_0}, the lift coefficient perpendicular to the local relative wind. The values of c_{l_0} and c_{d_0}, which are perpendicular and parallel to the local relative wind, may then be resolved into either chord and beam or any other directions; the fore-and-aft loads are thus obtained without the explicit use of a section induced drag. The angle that the local relative wind makes with the zero-lift direction is obtained by dividing c_{l_0} by m_0. In actual practice a portion of the wing is intercepted by the fuselage so that the actual span load distribution may be modified, depending upon whether or not the fuselage carries its proportionate share of the load. As so few data on fuselage loads are at present available, it may be assumed that for conventional cases the fuselage carries an amount of load equal to the load that would be carried by the wing it displaces.

LANGLEY MEMORIAL AERONAUTICAL LABORATORY,
NATIONAL ADVISORY COMMITTEE FOR AERONAUTICS,
LANGLEY FIELD, VA., *November 21, 1936.*

REFERENCES

1. Anderson, Raymond F.: Determination of the Characteristics of Tapered Wings. T. R. No. 572, N. A. C. A., 1936.
2. Wenzinger, Carl J., and Harris, Thomas A.: Pressure Distribution over a Rectangular Airfoil with a Partial-Span Split Flap. T. R. No. 571, N. A. C. A., 1936.
3. Lotz, Irmgard: Berechnung der Auftriebsverteilung beliebig geformter Flügel. Z. F. M., vol. 22, no. 7, April 14, 1931, S. 189–195.
4. Lippisch, A.: Method for the Determination of the Spanwise Lift Distribution. T. M. No. 778, N. A. C. A., 1935.
5. Parsons, John F.: Span Load Distribution on a Tapered Wing as Affected by Partial-Span Flaps from Tests in the Full-Scale Tunnel. Jour. Aero. Sciences, vol. 3, no. 5, March 1936, pp. 161–164.
6. Wenzinger, Carl J.: The Effect of Partial-Span Split Flaps on the Aerodynamic Characteristics of a Clark Y Wing. T. N. No. 472, N. A. C. A., 1933.
7. Wenzinger, Carl J.: The Effects of Full-Span and Partial-Span Split Flaps on the Aerodynamic Characteristics of a Tapered Wing. T. N. No. 505, N. A. C. A., 1934.
8. Shenstone, B. S.: The Lotz Method for Calculating the Aerodynamic Characteristics of Wings. R. A. S. Jour., vol. XXXVIII, no. 281, May 1934, pp. 432–444.
9. Lachmann, G. V.: Stalling of Tapered Wings. Flight, vol. XXIX, no. 1410, Jan. 2, 1936, pp. 10–13.

PLATE I.—COMPUTING FORM FOR EVALUATING ANGLE COEFFICIENTS, B_n

10 POINTS

y_1 y_2 y_3 y_4 y_5 y_6 y_7 y_8 y_9 $\frac{1}{2}y_{10}$

$y_1+y_3-y_5-y_7+y_9=r_1$ $y_2-y_6+\frac{1}{2}y_{10}=r_2$

Multiply	by									
Sin 9=0.1564	y_1		$-y_7$				$-y_3$		y_9	
Sin 18=0.3090		y_2		y_6				y_6		y_2
Sin 27=0.4540	y_3		y_1				$-y_9$		$-y_7$	
Sin 36=0.5878		y_4		$-y_8$				y_8		$-y_4$
Sin 45=0.7071	y_5		y_5		r_1		$-y_5$		y_5	
Sin 54=0.8090		y_6		y_2				y_2		y_6
Sin 63=0.8910	y_7		$-y_9$				y_1		$-y_3$	
Sin 72=0.9511		y_8		y_4				$-y_4$		$-y_8$
Sin 81=0.9877	y_9		y_3				y_7		y_1	
Sin 90=1.0000		$\frac{1}{2}y_{10}$		$-\frac{1}{2}y_{10}$		r_2		$-\frac{1}{2}y_{10}$		$\frac{1}{2}y_{10}$
Sum col. 1										
Sum col. 2										
Col. 1+col. 2		$=5B_1$		$=5B_3$		$=5B_5$		$=5B_7$		$=5B_9$
Col. 1−col. 2		$=5B_{19}$		$=5B_{17}$		$=5B_{15}$		$=5B_{13}$		$=5B_{11}$

Check: $B_1-B_3+B_5-B_7+B_9-B_{11}+B_{13}-B_{15}+B_{17}-B_{19}=y_{10}$.
NOTE.—If α_a is constant along the span, $B_1=\alpha_a$ and B_3 to B_{19} are 0.

PLATE II.—COMPUTING FORM FOR EVALUATING PLAN FORM COEFFICIENTS, C_{2n}

10 POINTS

	$\frac{1}{2}y_{10}'$	y_1' / y_9'	y_2' / y_8'	y_3' / y_7'	y_4' / y_6'	y_5'	v_0 / v_5	v_1 / v_4	v_2 / v_3
Sum	v_0	v_1	v_2	v_3	v_4	v_5	p_0	p_1	p_2
Difference	w_0	w_1	w_2	w_3	w_4		q_0	q_1	q_2

$10\ C_0=p_0+p_1+p_2$
$5\ C_{10}=w_0-w_2+w_4$
$10\ C_{20}=q_0-q_1+q_2$

Multiply	by							
Sin 18=0.3090	w_4		q_2	p_2	$-w_2$		p_1	$-q_1$
Sin 36=0.5878		w_3				w_1		
Sin 54=0.8090	w_2		q_1	$-p_1$	$-w_4$		$-p_2$	$-q_2$
Sin 72=0.9511		w_1				w_3		
Sin 90=1.00000	w_0		q_0	p_0	w_0		p_0	q_0
Sum col. 1								
Sum col. 2			$=5C_4$	$=5C_{16}$			$=5C_8$	$=5C_{12}$
Col. 1+col. 2		$=5C_2$				$=5C_6$		
Col. 1−col. 2		$=5C_{18}$				$=5C_{14}$		

Check: $C_0+C_2+C_4+C_6+C_8+C_{10}+C_{12}+C_{14}+C_{16}+C_{18}+C_{20}=0$.

PLATE III.—COMPUTING FORM FOR EVALUATING ANGLE COEFFICIENTS, B_n

20 POINTS

y_1 y_2 y_3 y_4 y_5 y_6 y_7 y_8 y_9 y_{10} y_{11} y_{12} y_{13} y_{14} y_{15} y_{16} y_{17} y_{18} y_{19} $\frac{1}{2}y_{20}$

$$y_1+y_7-y_9-y_{15}+y_{17}=r_1$$
$$y_2+y_6-y_{10}-y_{14}+y_{18}=r_2$$
$$y_3+y_5-y_{11}-y_{13}+y_{19}=r_3$$
$$y_4-y_{12}+\frac{1}{2}y_{20}\qquad=r_4$$

Multiply	by																			
Sin 4.5=0.0785	y_1		y_{13}		------------		y_{17}		y_9		$-y_{11}$		y_3		------------		y_7		$-y_{19}$	
Sin 9.0=0.1564		y_2		$-y_{14}$	------------			$-y_6$		y_{18}		y_{18}		$-y_6$	------------			$-y_{14}$		y_2
Sin 13.5=0.2334	y_3		y_1		------------		$-y_{11}$		y_{13}		$-y_7$		y_9		------------		y_{19}		y_{17}	
Sin 18.0=0.3090		y_4		y_{12}	------------			y_{12}		y_4		$-y_4$		$-y_{12}$	------------			$-y_{12}$		$-y_4$
Sin 22.5=0.3827	y_5		$-y_{15}$		r_1		y_5		$-y_5$		y_{15}		y_{15}		$-r_3$		y_5		$-y_{15}$	
Sin 27.0=0.4540		y_6		y_2	------------			$-y_{18}$		$-y_{14}$		$-y_{14}$		$-y_{18}$	------------			y_2		y_6
Sin 31.5=0.5225	y_7		y_{11}		------------		y_1		$-y_{17}$		y_3		y_{19}		------------		$-y_9$		y_{13}	
Sin 36.0=0.5878		y_8		$-y_{16}$	------------			y_{16}		$-y_8$		y_8		$-y_{16}$	------------			y_{16}		$-y_8$
Sin 40.5=0.6494	y_9		y_3		------------		$-y_7$		y_1		$-y_{19}$		y_{13}		------------		$-y_{17}$		$-y_{11}$	
Sin 45.0=0.7071		y_{10}		y_{10}		r_2		$-y_{10}$		y_{10}		y_{10}		$-y_{10}$		r_2		y_{10}		y_{10}
Sin 49.5=0.7604	y_{11}		$-y_{17}$		------------		y_{13}		y_{19}		y_1		y_7		------------		$-y_3$		y_9	
Sin 54.0=0.8090		y_{12}		y_4	------------			y_4		y_{12}		$-y_{12}$		$-y_4$	------------			$-y_4$		$-y_{12}$
Sin 58.5=0.8526	y_{13}		y_9		------------		$-y_{19}$		y_3		y_{17}		y_1		------------		y_{11}		$-y_7$	
Sin 63.0=0.8910		y_{14}		$-y_{18}$	------------			y_2		$-y_6$		$-y_6$		y_2	------------			$-y_{18}$		y_{14}
Sin 67.5=0.9239	y_{15}		y_5		r_3		y_{15}		$-y_{15}$		$-y_5$		$-y_5$		r_1		y_{15}		y_5	
Sin 72.0=0.9511		y_{16}		y_8	------------			$-y_8$		$-y_{16}$		y_{16}		y_8	------------			$-y_8$		$-y_{16}$
Sin 76.5=0.9724	y_{17}		$-y_{19}$		------------		$-y_9$		$-y_7$		$-y_{13}$		$-y_{11}$		------------		y_1		$-y_3$	
Sin 81.0=0.9877		y_{18}		y_6	------------			y_{14}		y_2		y_2		y_{14}	------------			y_6		y_{18}
Sin 85.5=0.9969	y_{19}		y_7		------------		y_3		y_{11}		y_9		$-y_{17}$		------------		$-y_{13}$		y_1	
Sin 90.0=1.0000		$\frac{1}{2}y_{20}$		$-\frac{1}{2}y_{20}$		r_4		$-\frac{1}{2}y_{20}$		$\frac{1}{2}y_{20}$		$-\frac{1}{2}y_{20}$		$\frac{1}{2}y_{20}$		$-r_4$		$\frac{1}{2}y_{20}$		$-\frac{1}{2}y_{20}$
Sum col. 1																				
Sum col. 2																				
Col. 1+col. 2		$10B_1$		$10B_3$		$10B_5$		$10B_7$		$10B_9$		$10B_{11}$		$10B_{13}$		$10B_{15}$		$10B_{17}$		$10B_{19}$
Col. 1−col. 2		$10B_{39}$		$10B_{37}$		$10B_{35}$		$10B_{33}$		$10B_{31}$		$10B_{29}$		$10B_{27}$		$10B_{25}$		$10B_{23}$		$10B_{21}$

Check: $B_1-B_3+B_5-B_7+B_9-\ \dots\ +\ \dots\ B_{39}=y_{20}$.

PLATE IV.—COMPUTING FORM FOR EVALUATING PLAN FORM COEFFICIENTS, C_{2n}

20 POINTS

		y_1'	y_2'	y_3'	y_4'	y_5'	y_6'	y_7'	y_8'	y_9'	y_{10}'
	$\frac{1}{2}y_{20}'$	y_{19}'	y_{18}'	y_{17}'	y_{16}'	y_{15}'	y_{14}'	y_{13}'	y_{12}'	y_{11}'	
Sum	v_0	v_1	v_2	v_3	v_4	v_5	v_6	v_7	v_8	v_9	v_{10}
Difference	w_0	w_1	w_2	w_3	w_4	w_5	w_6	w_7	w_8	w_9	

	v_0	v_1	v_2	v_3	v_4	v_5		p_0	p_1	p_2
	v_{10}	v_9	v_8	v_7	v_6			p_5	p_4	p_3
Sum	p_0	p_1	p_2	p_3	p_4	p_5		r_0	r_1	r_2
Difference	q_0	q_1	q_2	q_3	q_4			s_0	s_1	s_2

$$20\ C_0 = p_0+p_1+p_2+p_3+p_4+p_5$$
$$10\ C_{10} = \sqrt{2}(w_1-w_3-w_5+w_7+w_9)+w_0-w_4+w_8$$
$$10\ C_{20} = q_0-q_2+q_4$$
$$10\ C_{30} = \sqrt{2}(-w_1+w_3+w_5-w_7-w_9)+w_0-w_4+w_8$$
$$20\ C_{40} = p_0-p_1+p_2-p_3+p_4-p_5$$

Multiply	by															
	col. 1	col. 2	col. 1	col. 2	col. 1	col. 2	col. 1	col. 2	col. 1	col. 2	col. 1	col. 2				
Sin 9=0.1564		w_9				w_3				w_7		w_1				
Sin 18=0.3090	w_8		q_4		$-w_4$		$-q_2$		$-w_4$		w_8		s_2	r_1	$-s_1$	r_2
Sin 27=0.4540		w_7				$-w_9$				w_1		$-w_3$				
Sin 36=0.5878	w_6			q_3	w_2			q_1	$-w_2$		$-w_6$					
Sin 45=0.7071		w_5				$-w_5$				w_5		w_5				
Sin 54=0.8090	w_4		q_2		$-w_8$		$-q_4$		$-w_8$		w_4		s_1	$-r_2$	$-s_2$	$-r_1$
Sin 63=0.8910		w_3				w_1				$-w_9$		$-w_7$				
Sin 72=0.9511	w_2			q_1	$-w_6$			$-q_3$	w_6		$-w_2$					
Sin 81=0.9877		w_1				$-w_7$				$-w_3$		w_9				
Sin 90=1.0000	w_0		q_0		w_0		q_0		w_0		w_0		s_0	r_0	s_0	r_0
Sum col. 1													$10C_8$	$10C_{16}$	$10C_{24}$	$10C_{32}$
Sum col. 2																
Col. 1+col. 2		$10C_2$		$10C_4$		$10C_6$		$10C_{12}$		$10C_{14}$		$10C_{18}$				
Col. 1−col. 2		$10C_{38}$		$10C_{36}$		$10C_{34}$		$10C_{28}$		$10C_{26}$		$10C_{22}$				

Check: $C_0+C_2+c_4 \ldots C_{40}=0$.

TABLE I.—VALUES OF L_a FOR TAPERED WINGS WITH ROUNDED TIPS

	$A=6$										$A=10$										
λ \ $\frac{y}{b/2}$	0	0.15	0.30	0.45	0.60	0.70	0.80	0.90	0.95	0.975	0	0.15	0.30	0.45	0.60	0.70	0.80	0.90	0.95	0.975	$\frac{y}{b/2}$ / λ
1.00	1.164	1.163	1.144	1.115	1.050	0.987	0.870	0.669	0.485	0.358	1.116	1.111	1.106	1.090	1.052	1.011	0.929	0.757	0.572	0.433	1.00
.75	1.217	1.204	1.167	1.112	1.026	.953	.840	.648	.468	.340	1.194	1.179	1.140	1.089	1.020	.964	.875	.710	.536	.396	.75
.50	1.291	1.263	1.191	1.107	.995	.908	.789	.607	.447	.319	1.292	1.257	1.184	1.093	.982	.903	.800	.648	.492	.367	.50
.25	1.392	1.349	1.243	1.118	.954	.841	.709	.521	.386	.286	1.424	1.368	1.247	1.104	.940	.823	.695	.528	.407	.308	.25

TABLE II.—VALUES OF L_b FOR TAPERED WINGS WITH ROUNDED TIPS

[Values of L_b given for flaps at center. Reverse signs when using for flaps at tips]

Flaps at center	$\frac{b_f}{b_w}$ \ $\frac{y/b}{2}$	A=6: 0	0.15	0.30	0.45	0.60	0.70	0.80	0.90	0.95	0.975	A=10: 0	0.15	0.30	0.45	0.60	0.70	0.80	0.90	0.95	0.975	$\frac{y/b}{2}$ / $\frac{b_f}{b_w}$	Flaps at tip
	λ=1.00																						
	0.233	0.400	0.332	-0.002	-0.117	-0.147	-0.155	-0.145	-0.116	-0.085	-0.061	0.487	0.415	-0.023	-0.146	-0.173	-0.181	-0.170	-0.140	-0.107	-0.077	0.767	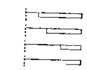
	.383	.351	.334	.238	-.112	-.221	-.236	-.227	-.185	-.139	-.100	.423	.405	.305	-.145	-.266	-.283	-.277	-.231	-.175	-.126	.617	
	.649	.192	.189	.169	.133	.006	-.251	-.313	-.275	-.209	-.157	.232	.229	.211	.178	.033	-.317	-.402	-.360	-.280	-.210	.351	
	.760	.110	.109	.106	.093	.060	-.013	-.255	-.289	-.230	-.171	.150	.147	.137	.117	.081	.001	-.340	-.386	-.307	-.227	.240	
	λ=0.75																						
	0.233	0.406	0.341	-0.004	-0.120	-0.148	-0.154	-0.143	-0.113	-0.083	-0.059	0.509	0.423	-0.027	-0.155	-0.177	-0.181	-0.174	-0.141	-0.107	-0.077	0.767	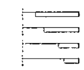
	.383	.353	.333	.236	-.114	-.218	-.233	-.222	-.180	-.134	-.096	.433	.414	.301	-.156	-.272	-.283	-.274	-.229	-.174	-.125	.617	
	.649	.192	.186	.164	.125	.006	-.245	-.305	-.266	-.204	-.149	.235	.230	.206	.169	.027	-.314	-.391	-.352	-.275	-.203	.351	
	.760	.118	.114	.104	.084	.046	-.021	-.248	-.273	-.213	-.155	.150	.147	.133	.112	.074	-.001	-.327	-.373	-.298	-.223	.240	
	λ=0.50																						
	0.233	0.420	0.340	-0.008	-0.124	-0.151	-0.153	-0.141	-0.111	-0.082	-0.059	0.534	0.436	-0.038	-0.167	-0.183	-0.182	-0.169	-0.140	-0.107	-0.077	0.767	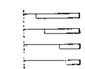
	.383	.360	.335	.227	-.123	-.221	-.230	-.218	-.176	-.134	-.096	.447	.424	.297	-.170	-.277	-.281	-.266	-.224	-.171	-.124	.617	
	.649	.191	.182	.159	.118	.002	-.240	-.295	-.256	-.197	-.146	.234	.226	.198	.159	.021	-.308	-.375	-.332	-.260	-.192	.351	
	.760	.118	.112	.100	.078	.043	-.022	-.240	-.263	-.206	-.150	.148	.141	.126	.103	.065	-.004	-.305	-.352	-.281	-.207	.240	
	λ=0.25																						
	0.233	0.425	0.342	-0.016	-0.136	-0.154	-0.151	-0.133	-0.106	-0.079	-0.058	0.558	0.445	-0.051	-0.186	-0.191	-0.183	-0.161	-0.129	-0.100	-0.075	0.767	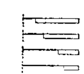
	.383	.361	.336	.222	-.134	-.225	-.226	-.205	-.164	-.124	-.090	.454	.425	.285	-.193	-.285	-.276	-.247	-.200	-.154	-.113	.617	
	.649	.186	.175	.149	.108	-.006	-.231	-.272	-.234	-.179	-.131	.223	.213	.183	.138	.004	-.266	-.335	-.287	-.228	-.173	.351	
	.760	.109	.104	.092	.070	.035	-.023	-.221	-.237	-.186	-.139	.133	.126	.112	.089	.052	-.009	-.278	-.300	-.241	-.183	.240	

TABLE III.—CALCULATION OF LIFT DISTRIBUTION FOR ILLUSTRATIVE EXAMPLE

[A, 6; b_f/b_w, 0.383; S, 266.7 sq. ft.; b, 40 ft.; λ, 0.625; C_L, 1.72; Δc_l, 0.60; q, 57.5]

1	2	3	4	5	6	7	8	9
Station $y/\frac{b}{2}$	Chord (ft.)	L_a	L_b	$c_{l_{a1}}$	c_{l_a}	c_{l_b}	c_l	l (lb.)
0	8.500	1.254	0.356	0.984	1.693	0.168	1.861	91.0
.15	8.022	1.233	.334	1.025	1.762	.167	1.929	89.0
.30	7.544	1.179	.232	1.043	1.794	.123	1.917	83.1
.45	7.066	1.110	−.118	1.047	1.801	−.067	1.734	70.5
.60	6.588	1.010	−.220	1.022	1.758	−.134	1.624	61.6
.70	6.269	.930	−.232	.989	1.700	−.148	1.552	56.0
.80	5.820	.815	−.220	.934	1.607	−.151	1.456	48.7
.90	4.825	.628	−.179	.868	1.492	−.148	1.344	37.3
.95	3.655	.457	−.134	.835	1.435	−.147	1.288	27.1
.975	2.635	.330	−.097	.835	1.435	−.147	1.288	19.5

TABLE IV.—CIRCULATION COEFFICIENTS

[A, 6; λ, 1.0; b_f/b_w, 0.649]

No flaps				Flaps at center			
Coefficient	4 harmonics retained	6 harmonics retained	10 harmonics retained	Coefficient	4 harmonics retained	6 harmonics retained	10 harmonics retained
A_1	0.9280	0.9290	0.9290	A_1	0.6682	0.6684	0.6682
A_3	.1158	.1160	.1161	A_3	−.1825	−.1826	−.1826
A_5	.0251	.0251	.0251	A_5	−.0298	−.0301	−.0300
A_7	.0069	.0072	.0073	A_7	.0588	.0585	.0586
A_9	----------	.0026	.0026	A_9	----------	.0017	.0019
A_{11}	----------	.0011	.0011	A_{11}	----------	−.0286	−.0281
A_{13}	----------	----------	.0005	A_{13}	----------	----------	.0058
A_{15}	----------	----------	.0003	A_{15}	----------	----------	.0168
A_{17}	----------	----------	.0002	A_{17}	----------	----------	−.0083
A_{19}	----------	----------	.0004	A_{19}	----------	----------	−.0104

TABLE V.—GEOMETRIC CHARACTERISTICS OF WING USED IN EXAMPLE

1	2	3	4	5	6	7	8	9	10
A	Fraction of semispan	θ (deg.)	$\sin\theta$	α (rad.)	$\alpha\sin\theta$	m_0 for $b=\infty$	$\frac{m_s}{m_0}$	$\frac{c_s}{c}$	$\frac{m_s c_s}{m_0 c}\sin\theta$
20	0	90	1.0000	1	1.0000	5.67	1.0	1.0000	1.0000
19	.0785	85.5	.9969	1	.9969	5.67	1.0	1.0400	1.0370
18	.1564	81	.9877	1	.9877	5.67	1.0	1.0848	1.0717
17	.2334	76.5	.9724	1	.9724	5.67	1.0	1.1295	1.1030
16	.3090	72	.9511	1	.9511	5.67	1.0	1.1827	1.1252
15	.3827	67.5	.9239	1	.9239	5.67	1.0	1.2386	1.1445
14	.4540	63	.8910	1	.8910	5.67	1.0	1.2937	1.1530
13	.5225	58.5	.8526	0	0	5.67	1.0	1.3555	1.1560
12	.5878	54	.8090	0	0	5.67	1.0	1.4162	1.1455
11	.6494	49.5	.7604	0	0	5.67	1.0	1.4785	1.1245
10	.7071	45	.7071	0	0	5.67	1.0	1.5469	1.0939
9	.7604	40.5	.6494	0	0	5.67	1.0	1.6100	1.0458
8	.8090	36	.5878	0	0	5.67	1.0	1.6793	.9869
7	.8526	31.5	.5225	0	0	5.67	1.0	1.7415	.9100
6	.8910	27	.4540	0	0	5.67	1.0	1.8219	.8272
5	.9239	22.5	.3827	0	0	5.67	1.0	1.9605	.7500
4	.9511	18	.3090	0	0	5.67	1.0	2.2504	.6953
3	.9724	13.5	.2334	0	0	5.67	1.0	2.8280	.6600
2	.9877	9	.1564	0	0	5.67	1.0	4.0742	.6372
1	.9969	4.5	.0785	0	0	5.67	1.0	7.9740	.6260
0	1.0000	0	0	0	0	5.67	1.0	----------	----------

TABLE VI.—COMPUTATION OF ANGLE COEFFICIENTS, B_n

y_1	y_2	y_3	y_4	y_5	y_6	y_7	y_8	y_9	y_{10}	y_{11}	y_{12}	y_{13}	y_{14}	y_{15}	y_{16}	y_{17}	y_{18}	y_{19}	$\frac{1}{2}y_{20}$
0	0	0	0	0	0	0	0	0	0	0	0	0	0.8910	0.9239	0.9511	0.9724	0.9877	0.9969	0.5000

$r_1=0+0-0-0.9239+0.9724=0.0485$
$r_2=0+0-0-0.8910+0.9877=\ .0967$
$r_3=0+0-0-0\quad +0.9969=\ .9969$
$r_4=0-0+0.5000\quad =\ .5000$

Multiply	by									
Sin 4.5=0.0785	0	0		0.0763	0	0	0		0	−0.0783
Sin 9 =0.1564	0	−0.1394		0	0.1545	0.1545	0		−0.1394	0
Sin 13.5=0.2334	0	0		0	0	0	0		0.2327	.2270
Sin 18 =0.3090	0	0		0	0	0	0		0	0
Sin 22.5=0.3827	0	−0.3536	0.0186	0	0	0.3536	0.3536	−0.3815	0	−.3536
Sin 27 =0.4540	0	0		−0.4484	−.4045	−.4045	−0.4484		0	0
Sin 31.5=0.5225	0	0		0	−0.5081	0	.5209		0	0
Sin 36 =0.5878	0	−.5591		.5591	0	0	−.5591		.5591	0
Sin 40.5=0.6494	0	0		0	0	−.6474	0		−.6315	0
Sin 45 =0.7071	0	0	0.0684	0	0	0	0	0.0684	0	0
Sin 49.5=0.7604	0	−.7394		0	.7580	0	0		0	0
Sin 54 =0.8090	0	0		0	0	0	0		0	0
Sin 58.5=0.8526	0	0		−.8500	0	.8291	0		0	0
Sin 63 =0.8910	.7939	−.8800		0	0	0	0		−.8800	0.7939
Sin 67.5=0.9239	.8536	0	.9210	.8536	−.8536	0	0	.0448	.8536	0
Sin 72 =0.9511	.9046	0		0	−.9046	.9046	0		0	−.9046
Sin 76.5=0.9724	.9456	−.9694		0	0	0	0		0	0
Sin 81 =0.9877	.9756	0		.8800	0	0	.8800		0	.9756
Sin 85.5=0.9969	.9938	0		0	0	0	−.9694		(	0
Sin 90 =1.0000	.5000	−.5000	.5000	−.5000	.5000	−.5000	.5000	−.5000	.5000	−.5000
Sum col. 1	2.7930	−2.0624	0.9396	0.0799	−0.6037	0.5353	−0.0949	−0.3367	0.4548	−0.2049
Sum col. 2	3.1741	−2.0785	.5684	.4907	−.6546	.1546	.3725	−.4316	.0397	.3649
Col. 1+col. 2	5.9671=10B_1	−4.1409=10B_3	1.5080=10B_5	0.5706=10B_7	−1.2583=10B_9	0.6899=10B_{11}	0.2776=10B_{13}	−0.7683=10B_{15}	0.4945=10B_{17}	0.1600=10B_{19}
Col. 1−col. 2	−.3811=10B_{39}	.0161=10B_{37}	.3712=10B_{35}	−.4108=10B_{33}	.0509=10B_{31}	.3807=10B_{29}	−.4674=10B_{27}	.0949=10B_{25}	.4151=10B_{23}	−.5698=10B_{21}

Check:

$B_1 - B_3 + B_5 - B_7 + B_9 - B_{11} + B_{13} - B_{15} + B_{17} - B_{19} + B_{21} - B_{23} + B_{25} - B_{27} + B_{29} - B_{31} + B_{33} - B_{35} + B_{37} - B_{39} = y_{20}.$
$0.5967+0.4141+0.1508-0.0571-0.1258-0.0690+0.0278+0.0768+0.0495-0.0160-0.0570-0.0415+0.0095+0.0467+0.0381-0.0051-0.0411-0.0371+0.0016+0.0381=1.0000.$

COMPUTION OF PLAN-FORM COEFFICIENTS, C_{2n}

		0. 6260	0. 6372	0. 6600	0. 6953	0. 7500	0. 8272	0. 9100	0. 9869	1. 0458	1. 0939
	0. 5000	1. 0370	1. 0717	1. 1030	1. 1252	1. 1445	1. 1530	1. 1560	1. 1455	1. 1245	
Sum	0. 5000	1. 6630	1. 7089	1. 7630	1. 8205	1. 8945	1. 9802	2. 0660	2. 1324	2. 1703	1. 0939
Difference	−. 5000	−. 4110	−. 4345	−. 4430	−. 4299	−. 3945	−. 3258	−. 2460	−. 1586	−. 0787	1. 0939

	0. 5000	1. 6630	1. 7089	1. 7630	1. 8205	1. 8945	1. 5939	3. 8333	3. 8413
	1. 0939	2. 1703	2. 1324	2. 0660	1. 9802		1. 8945	3. 8007	3. 8290
Sum	1. 5939	3. 8333	3. 8413	3. 8290	3. 8007	1. 8945	3. 4884	7. 6340	7. 6703
Difference	−. 5939	−. 5073	−. 4235	−. 3030	−. 1597		−. 3006	. 0326	. 0123

$20C_0=1.5939+3.8333+3.8413+3.8290+3.8007+1.8945=18.7927$
$10C_{10}=1.4142(-0.4110+0.4430+0.3945-0.2460-0.0787)-0.5000+0.4299-0.1586=-0.0847$
$10C_{20}=-0.5939+0.4235-0.1597=-0.3301$
$10C_{30}=1.4142(0.4110-0.4430-0.3945+0.2460+0.0787)-0.5000+0.4299-0.1586=-0.3727$
$20C_{40}=1.5939-3.8333+3.8413-3.8290+3.8007-1.8945=-0.3209$

Multiply	by									
Sin 9=0.1564	−0. 0123		−0. 0693		−0. 0385	−0. 0643				
Sin 18=0.3090	−0. 0490	−0. 0493	0. 1328	0. 1309	0. 1328	−0. 0490	0. 0038	2. 3589	−0. 0101	2. 3701
Sin 27=0.4540	−. 1117		. 0357		−. 1866	. 2011				
Sin 36=0.5878	−. 1915	−0. 1781	−. 2554	−0. 2982	. 2554	. 1915				
Sin 45=0.7071	−. 2790		. 2790		−. 2790	−. 2790				
Sin 54=0.8090	−. 3478	−. 3426	. 1283	. 1292	. 1283	−. 3478	. 0264	−6. 2053	−. 0100	−6. 1759
Sin 63=0.8910	−. 3947		−. 3662		. 0701	. 2192				
Sin 72=0.9511	−. 4133	−. 4825	. 3099	. 2882	−. 3099	. 4133				
Sin 81=0.9877	−. 4059		. 2430		. 4376	−. 0777				
Sin 90=1.0000	−. 5000	−. 5939	−. 5000	−. 5939	−. 5000	−. 5000	−. 3006	3. 4884	−. 3006	3. 4884
Sum col. 1	−1. 5016	−. 9858	−. 1844	−. 3338	−. 2934	−. 2920	−. 2704	−. 3580	−. 3207	−. 3174
Sum col. 2	−1. 2036	−. 6606	. 1222	−. 0100	. 0036	−. 0007	10 C_8	10 C_{16}	10 C_{24}	10 C_{32}
Col. 1+col. 2	−2. 7052=10 C_2	−1. 6464=10 C_4	−. 0622=10 C_6	−. 3438=10 C_{12}	−. 2898=10 C_{14}	−. 2927=10 C_{18}	----------	----------	----------	----------
Col. 1−col. 2	−. 2980=10 C_{38}	−. 3252=10 C_{36}	−. 3066=10 C_{34}	−. 3238=10 C_{28}	−. 2970=10 C_{26}	−. 2913=10 C_{22}	----------	----------	----------	----------

Check: $0.9396-0.2705-0.1646-0.0062-0.0270-0.0085-0.0344-0.0290-0.0358-0.0293-0.0330-0.0291-0.0321-0.0297-0.0324-0.0373-0.0317-0.0307-0.0325-0.0298-0.0160=0.$

TABLE VII.—SOLUTION OF A_n COEFFICIENTS

1	2	3 (a)	3 (b)	3 (c)	4 (a)	4 (b)	4 (c)
$(C_2-C_4)A_3$	−0.1059		−0.2563	−0.2487		0.0271	0.0263
$(C_4-C_6)A_5$	−.1584		.0824	.0823		−.0131	−.0130
$(C_6-C_8)A_7$	.0208		.0182	.0169		.0004	.0004
$(C_8-C_{10})A_9$	−.0185		−.0411	−.0400		.0008	.0007
$(C_{10}-C_{12})A_{11}$	.0259		.0190	.0189		.0005	.0005
$(C_{12}-C_{14})A_{13}$	−.0054		.0092	.0087		0	0
$(C_{14}-C_{16})A_{15}$	.0068		−.0201	−.0197		−.0001	−.0001
$(C_{16}-C_{18})A_{17}$	−.0065		.0117	.0118		−.0001	−.0001
$(C_{18}-C_{20})A_{19}$	.0037		.0032	.0032		0	0
Σ					0	.0155	.0147
$\Sigma/2$					0	.0077	.0073
$B_1-\Sigma/2$	.5967				.5967	.5890	.5894
$A_1=\frac{(B_1-\Sigma/2)}{P_1}$	/1.2667				.4711	.4650	.4653
$(C_2-C_4)A_1$	−0.1059	0.4711	0.4650	0.4653	−0.0499	−0.0492	−0.0493
$(C_2-C_8)A_5$	−.2435		.0824	.0823		−.0201	−.0200
$(C_4-C_{10})A_7$	−.1561		.0182	.0169		−.0028	−.0026
$(C_6-C_{12})A_9$	.0282		−.0411	−.0400		−.0012	−.0011
$(C_8-C_{14})A_{11}$	.0020		.0190	.0189		0	0
$(C_{10}-C_{16})A_{13}$	.0273		.0092	.0087		.0002	.0002
$(C_{12}-C_{18})A_{15}$	−.0051		−.0201	−.0197		.0001	.0001
$(C_{14}-C_{20})A_{17}$	.0040		.0117	.0118		.0001	.0001
$(C_{16}-C_{22})A_{19}$	−.0067		.0032	.0032		0	0
Σ					−.0499	−.0730	−.0726
$\Sigma/2$					−.0249	−.0365	−.0363
$B_3-\Sigma/2$	−.4141				−.3892	−.3776	−.3778
$A_3=\frac{(B_3-\Sigma/2)}{P_3}$	/1.5185				−.2563	−.2487	−.2488
$(C_4-C_6)A_1$	−0.1584	0.4711	0.4650	0.4653	−0.0746	−0.0736	0−.0737
$(C_2-C_8)A_3$	−.2435	−.2563	−.2487	−.2488	.0624	.0606	.0606
$(C_2-C_{12})A_7$	−.2361		.0182	.0169		−.0043	−.0041
$(C_4-C_{14})A_9$	−.1356		−.0411	−.0400		.0056	.0054
$(C_6-C_{16})A_{11}$	.0296		.0190	.0189		.0006	.0006
$(C_8-C_{18})A_{13}$	.0023		.0092	.0087		0	0
$(C_{10}-C_{20})A_{15}$	.0245		−.0201	−.0197		−.0005	−.0005
$(C_{12}-C_{22})A_{17}$	−.0053		.0117	.0118		−.0001	−.0001
$(C_{14}-C_{24})A_{19}$	.0031		.0032	.0032		0	0
Σ					−.0122	−.0117	−.0118
$\Sigma/2$					−.0061	−.0059	−.0059
$B_5-\Sigma/2$	.1508				.1569	.1567	.1567
$A_5=\frac{(B_5-\Sigma/2)}{P_5}$	/1.9035				.0824	.0823	.0823
$(C_6-C_8)A_1$	0.0280	0.4711	0.4650	0.4653	0.0098	0.0097	0.0097
$(C_4-C_{10})A_3$	−.1561	−.2563	−.2487	−.2488	.0400	.0388	.0388
$(C_2-C_{12})A_5$	−.2361	.0824	.0823	.0823	−.0195	−.0194	−.0194
$(C_2-C_{16})A_9$	−.2347		−.0411	−.0400		.0096	.0094
$(C_4-C_{18})A_{11}$	−.1353		.0190	.0189		−.0026	−.0026
$(C_6-C_{20})A_{13}$	.0268		.0092	.0087		.0002	.0002
$(C_8-C_{22})A_{15}$	.0021		−.0201	−.0197		0	0
$(C_{10}-C_{24})A_{17}$	.0236		.0117	.0118		.0003	.0003
$(C_{12}-C_{26})A_{19}$	−.0047		.0032	.0032		0	0
Σ					.0303	.0366	.0364
$\Sigma/2$					.0152	.0183	.0182
$B_7-\Sigma/2$	.0571				.0419	.0388	.0389
$A_7=\frac{(B_7-\Sigma/2)}{P_7}$	/2.2977				.0182	.0169	.0169
$(C_8-C_{10})A_1$	−0.0185	0.4711	0.4650	0.4653	−0.0087	−0.0086	−0.0086
$(C_6-C_{12})A_3$	.0282	−.2563	−.2487	−.2488	−.0072	−.0070	−.0070
$(C_4-C_{14})A_5$	−.1356	.0824	.0823	.0823	−.0112	−.0112	−.0112
$(C_2-C_{16})A_7$	−.2347	.0182	.0169	.0169	−.0043	−.0040	−.0040
$(C_2-C_{20})A_{11}$	−.2375		.0190	.0189		−.0045	−.0045
$(C_4-C_{22})A_{13}$	−.1355		.0092	.0087		−.0012	−.0012
$(C_6-C_{24})A_{15}$	.0259		−.0201	−.0197		−.0005	−.0005
$(C_8-C_{26})A_{17}$	.0027		.0117	.0118		0	0
$(C_{10}-C_{28})A_{19}$	.0239		.0032	.0032		.0001	.0001
Σ					−.0314	−.0369	−.0369
$\Sigma/2$					−.0157	−.0184	−.0184
$B_9-\Sigma/2$	−.1258				−.1101	−.1074	−.1074
$A_9=\frac{(B_9-\Sigma/2)}{P_9}$	/2.6817				−.0411	−.0400	−.0400
$(C_{10}-C_{12})A_1$	0.0259	0.4711	0.4650	0.4653	0.0122	0.0120	0.0120
$(C_8-C_{14})A_3$	.0020	−.2563	−.2487	−.2488	−.0005	−.0005	−.0005
$(C_6-C_{16})A_5$	.0296	.0824	.0823	.0823	.0024	.0024	.0024
$(C_4-C_{18})A_7$	−.1353	.0182	.0169	.0169	−.0025	−.0023	−.0023
$(C_2-C_{20})A_9$	−.2375	−.0411	−.0400	−.0400	.0098	.0095	.0095
$(C_2-C_{24})A_{13}$	−.2384		.0092	.0087		−.0022	−.0021
$(C_4-C_{26})A_{15}$	−.1349		−.0201	−.0197		.0027	.0027
$(C_6-C_{28})A_{17}$	.0262		.0117	.0118		.0003	.0003
$(C_8-C_{30})A_{19}$	.0103		.0032	.0032		0	0
Σ					.0214	.0219	.0220
$\Sigma/2$					.0107	.0110	.0110
$B_{11}-\Sigma/2$	.0690				.0583	.0580	.0580
$A_{11}=\frac{(B_{11}-\Sigma/2)}{P_{11}}$	/3.0654				.0190	.0189	.0189
$(C_{12}-C_{14})A_1$	−0.0054	0.4711	0.4650	0.4653	−0.0025	−0.0025	−0.0025
$(C_{10}-C_{16})A_3$	.0273	−.2563	−.2487	−.2488	−.0070	−.0068	−.0068
$(C_8-C_{18})A_5$	.0023	.0824	.0823	.0823	.0002	.0002	.0002
$(C_6-C_{20})A_7$	.0268	.0182	.0169	.0169	.0005	.0004	.0004
$(C_4-C_{22})A_9$	−.1355	−.0401	−.0400	−.0400	.0056	.0054	.0054
$(C_2-C_{24})A_{11}$	−.2384	.0190	.0189	.0189	−.0045	−.0045	−.0045
$(C_2-C_{28})A_{15}$	−.2381		−.0201	−.0197		.0048	.0047
$(C_4-C_{30})A_{17}$	−.1273		.0117	.0118		−.0015	−.0015
$(C_6-C_{32})A_{19}$	.0255		.0032	.0032		.0001	.0001
Σ					−.0077	−.0044	−.0045
$\Sigma/2$					−.0039	−.0022	−.0022
$B_{13}-\Sigma/2$	.0278				.0317	.0300	.0300
$A_{13}=\frac{(B_{13}-\Sigma/2)}{P_{13}}$	/3.4496				.0092	.0087	.0087
$(C_{14}-C_{16})A_1$	0.0068	0.4711	0.4650	0.4653	0.0032	0.0032	0.0032
$(C_{12}-C_{18})A_3$	−.0051	−.2563	−.2487	−.2488	.0013	.0013	.0013
$(C_{10}-C_{20})A_5$	.0245	.0824	.0823	.0823	.0020	.0020	.0020
$(C_8-C_{22})A_7$	.0021	.0182	.0169	.0169	0	0	0
$(C_6-C_{24})A_9$	.0259	−.0411	−.0400	−.0400	−.0011	−.0010	−.0010
$(C_4-C_{26})A_{11}$	−.1349	.0190	.0189	.0189	−.0026	−.0026	−.0026
$(C_2-C_{28})A_{13}$	−.2381	.0092	.0087	.0087	−.0022	−.0021	−.0021
$(C_2-C_{32})A_{17}$	−.2388		.0117	.0118		−.0028	−.0028
$(C_4-C_{34})A_{19}$	−.1339		.0032	.0032		−.0004	−.0004
Σ					.0006	−.0024	−.0024
$\Sigma/2$					.0003	−.0012	−.0012
$B_{15}-\Sigma/2$	−.0768				−.0771	−.0756	−.0756
$A_{15}=\frac{(B_{15}-\Sigma/2)}{P_{15}}$	/3.8373				−.0201	−.0197	−.0197
$(C_{16}-C_{18})A_1$	−0.0065	0.4711	0.4650	0.4653	−0.0031	−0.0030	−0.0030
$(C_{14}-C_{20})A_3$	.0040	−.2563	−.2487	−.2488	−.0010	−.0010	−.0010
$(C_{12}-C_{22})A_5$	−.0053	.0824	.0823	.0823	−.0004	−.0004	−.0004
$(C_{10}-C_{24})A_7$	.0236	.0182	.0169	.0169	.0004	.0004	.0004
$(C_8-C_{26})A_9$	.0027	−.0411	−.0400	−.0400	−.0001	−.0001	−.0001
$(C_6-C_{28})A_{11}$	.0262	.0190	.0189	.0189	.0005	.0005	.0005
$(C_4-C_{30})A_{13}$	−.1273	.0092	.0087	.0087	−.0012	−.0011	−.0011
$(C_2-C_{32})A_{15}$	−.2388	−.0201	−.0197	−.0197	.0048	.0047	.0047
$(C_2-C_{36})A_{19}$	−.2380		.0032	.0032		−.0008	−.0008
Σ					−.0001	−.0008	−.0008
$\Sigma/2$					0	−.0004	−.0004
$B_{17}-\Sigma/2$	.0494				.0494	.0498	.0498
$A_{17}=\frac{(B_{17}-\Sigma/2)}{P_{17}}$	/4.2180				.0117	.0118	.0118
$(C_{18}-C_{20})A_1$	0.0037	0.4711	0.4650	0.4653	0.0017	0.0017	0.0017
$(C_{16}-C_{22})A_3$	−.0067	−.2563	−.2487	−.2488	.0017	.0017	.0017
$(C_{14}-C_{24})A_5$	.0031	.0824	.0823	.0823	.0003	.0003	.0003
$(C_{12}-C_{26})A_7$	−.0047	.0182	.0169	.0169	−.0001	−.0001	−.0001
$(C_{10}-C_{28})A_9$	.0239	−.0411	−.0400	−.0400	−.0010	−.0010	−.0010
$(C_8-C_{30})A_{11}$	.0103	.0190	.0189	.0189	.0002	.0002	.0002
$(C_6-C_{32})A_{13}$	.0255	.0092	.0087	.0087	.0002	.0002	.0002
$(C_4-C_{34})A_{15}$	−.1339	−.0201	−.0197	−.0197	.0027	.0026	.0026
$(C_2-C_{36})A_{17}$	−.2380	.0117	.0118	.0118	−.0028	−.0028	−.0028
Σ					.0029	.0028	.0028
$\Sigma/2$					.0015	.0014	.0014
$B_{19}-\Sigma/2$	.0160				.0145	.0146	.0146
$A_{19}=\frac{(B_{19}-\Sigma/2)}{P_{19}}$	/4.6014				.0032	.0032	.0032

TABLE VIII.—COMPUTATION OF LOAD DISTRIBUTIONS

	20	18	16	14	12	10	8	6	4	2
θ, degrees	90	81	72	63	54	45	36	27	18	9
Sin θ	1.0000	0.9877	0.9511	0.8910	0.8090	0.7071	0.5878	0.4540	0 3090	0.1564
Sin 3θ	−1.0000	−.8910	−.5878	−.1564	.3090	.7071	.9511	.9877	.8090	.4540
Sin 5θ	1.0000	.7071	0	−.7071	−1.0000	−.7071	0	.7071	1.0000	.7071
Sin 7θ	−1.0000	−.4540	.5878	.9877	.3090	−.7071	−.9511	−.1564	.8090	.8910
Sin 9θ	1.0000	.1564	−.9511	−.4540	.8090	.7071	−.5878	−.8910	.3090	.9877
Sin 11θ	−1.0000	.1564	.9511	−.4540	−.8090	.7071	.5878	−.8910	−.3090	.9877
Sin 13θ	1.0000	−.4540	−.5878	.9877	−.3090	−.7071	.9511	−.1564	−.8090	.8910
Sin 15θ	−1.0000	.7071	0	−.7071	1.0000	−.7071	0	.7071	−1.0000	.7071
Sin 17θ	1.0000	−.8910	.5878	−.1564	−.3090	.7071	−.9511	.9877	−.8090	.4540
Sin 19θ	−1.0000	.9877	−.9511	.8910	−.8090	.7071	−.5878	.4540	−.3090	.1564
$A_1 \sin \theta$	.4653	.4596	.4425	.4146	.3764	.3290	.2735	.2112	.1438	.0728
$A_3 \sin 3\theta$	.2488	.2217	.1462	.0389	−.0769	−.1759	−.2366	−.2457	−.2013	−.1129
$A_5 \sin 5\theta$	.0823	.0582	0	−.0582	−.0823	−.0582	0	.0582	.0823	.0582
$A_7 \sin 7\theta$	−.0169	−.0077	.0099	.0167	.0052	−.0120	−.0161	−.0026	.0137	.0151
$A_8 \sin 9\theta$	−.0400	−.0063	.0381	.0182	−.0324	−.0283	.0235	.0357	−.0124	−.0396
$A_{11} \sin 11\theta$	−.0189	.0030	.0180	−.0086	−.0153	.0134	.0111	−.0168	−.0058	.0187
$A_{13} \sin 13\theta$	.0087	−.0039	−.0051	.0086	−.0027	−.0061	.0083	−.0014	−.0070	.0077
$A_{15} \sin 15\theta$	.0197	−.0139	0	.0139	−.0197	.0139	0	−.0139	.0197	−.0139
$A_{17} \sin 17\theta$	.0118	−.0105	.0069	−.0018	−.0037	.0084	−.0112	.0117	−.0096	.0054
$A_{19} \sin 19\theta$	−.0032	.0031	−.0030	.0028	−.0026	.0022	−.0019	.0014	−.0010	.0005
$\Sigma A_n \sin n\theta$	.7576	.7033	.6535	.4451	.1460	.0864	.0506	.0378	.0224	.0120
$m_s c_s / c$	5.670	6.152	6.708	7.337	8.029	8.772	9.520	10.331	12.760	23.100
$c_l = m_s c_s / c \times \Sigma()$	4.296	4.327	4.384	3.266	1.172	.7579	.4817	.3905	.2858	.2772
$A_1 \sin \theta$	.4653	.4596	.4425	.4146	.3764	.3290	.2735	.2112	.1438	.0728
$3A_3 \sin 3\theta$	.7463	.6650	.4387	.1167	−.2306	−.5277	−.7098	−.7371	−.6038	−.3388
$5A_5 \sin 5\theta$	.4115	.2910	0	−.2910	−.4115	−.2910	0	.2910	.4115	.2910
$7A_7 \sin 7\theta$	−.1184	−.0538	.0696	.1170	.0366	−.0837	−.1126	−.0185	.0958	.1055
$9A_9 \sin 9\theta$	−.3604	−.0564	.3428	.1636	−.2916	−.2549	.2119	.3212	−.1114	−.3560
$11A_{11} \sin 11\theta$	−.2078	.0325	.1976	−.0943	−.1681	.1469	.1221	−.1851	−.0642	.2052
$13A_{13} \sin 13\theta$	.1130	−.0513	−.0664	.1116	−.0349	−.0799	.1074	−.0177	−.0914	.1007
$15A_{15} \sin 15\theta$	.2957	−.2091	0	.2091	−.2957	.2091	0	−.2091	.2957	−.2091
$17A_{17} \sin 17\theta$	.2009	−.1790	.1181	−.0314	−.0621	.1421	−.1911	.1985	−.1626	.0912
$19A_{19} \sin 19\theta$	−.0602	.0595	−.0573	.0537	−.0487	.0426	−.0354	.0273	−.0186	.0094
$\Sigma n A_n \sin n\theta$	1.4859	.9580	1.4856	.7696	−1.1302	−.3675	−.3340	−.1183	−.1052	−.0281
$m_s c_s / 4b \times \Sigma() / \sin \theta$	.2852	.1839	.2851	.1477	−.2169	−.0705	−.0641	−.0227	−.0202	−.0054
$c_{d_i} = c_l \left[\frac{m_s c_s}{4b} \times \frac{\Sigma()}{\sin \theta} \right]$	1.2252	.7957	1.2499	.4824	−.2542	−.0534	−.0309	−.0089	−.0058	−.0015

U. S. GOVERNMENT PRINTING OFFICE: 1937

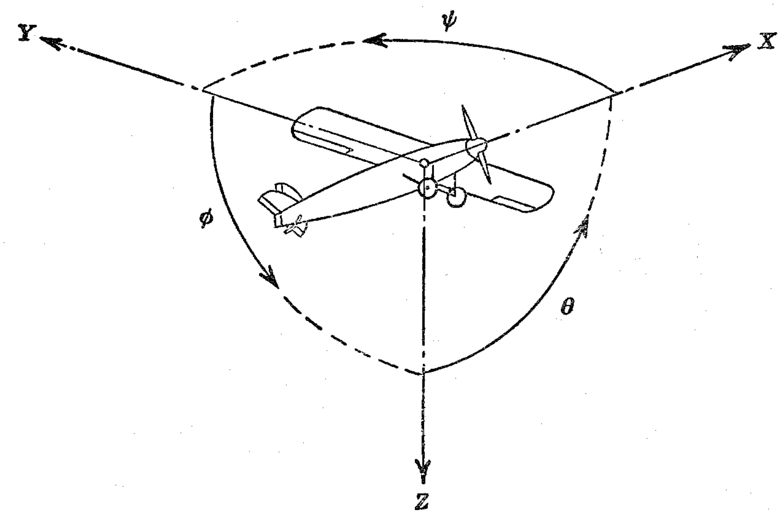

Positive directions of axes and angles (forces and moments) are shown by arrows

Axis		Force (parallel to axis) symbol	Moment about axis			Angle		Velocities	
Designation	Symbol		Designation	Symbol	Positive direction	Designation	Symbol	Linear (component along axis)	Angular
Longitudinal	X	X	Rolling	L	$Y \longrightarrow Z$	Roll	ϕ	u	p
Lateral	Y	Y	Pitching	M	$Z \longrightarrow X$	Pitch	θ	v	q
Normal	Z	Z	Yawing	N	$X \longrightarrow Y$	Yaw	ψ	w	r

Absolute coefficients of moment

$C_l = \frac{L}{qbS}$ (rolling) $\quad C_m = \frac{M}{qcS}$ (pitching) $\quad C_n = \frac{N}{qbS}$ (yawing)

Angle of set of control surface (relative to neutral position), δ. (Indicate surface by proper subscript.)

4. PROPELLER SYMBOLS

- D, Diameter
- p, Geometric pitch
- p/D, Pitch ratio
- V', Inflow velocity
- V_s, Slipstream velocity
- T, Thrust, absolute coefficient $C_T = \frac{T}{\rho n^2 D^4}$
- Q, Torque, absolute coefficient $C_Q = \frac{Q}{\rho n^2 D^5}$
- P, Power, absolute coefficient $C_P = \frac{P}{\rho n^3 D^5}$
- C_s, Speed-power coefficient $= \sqrt[5]{\frac{\rho V^5}{P n^2}}$
- η, Efficiency
- n, Revolutions per second, r.p.s.
- Φ, Effective helix angle $= \tan^{-1}\left(\frac{V}{2\pi rn}\right)$

5. NUMERICAL RELATIONS

1 hp. = 76.04 kg-m/s = 550 ft-lb./sec.
1 metric horsepower = 1.0132 hp.
1 m.p.h. = 0.4470 m.p.s.
1 m.p.s. = 2.2369 m.p.h.
1 lb. = 0.4536 kg.
1 kg = 2.2046 lb.
1 mi. = 1,609.35 m = 5,280 ft.
1 m = 3.2808 ft.